UNIVERSIDADE DE SÃO PAULO
INSTITUTO DE GEOCIÊNCIAS

Ore-genesis and evolution of the Pb-Zn-Ag-(Cu-Ba) deposits hosted by the Perau Formation, Southern Ribeira Belt, Brazil

ANDERSON DOURADO RODRIGUES DA SILVA

Dissertação apresentada ao Programa de Geociências (Mineralogia e Petrologia) para obtenção do título de Mestre em Ciências.

Área de concentração: Petrologia Ígnea e Metamórfica.

Orientador: Prof. Dr. Frederico Meira Faleiros

Serviço de Biblioteca e Documentação do IGc/USP

Ficha catalográfica gerada automaticamente com dados fornecidos pelo(a) autor(a) via programa desenvolvido pela Seção Técnica de Informática do ICMC/USP

Bibliotecários responsáveis pela estrutura de catalogação da publicação: Sonia Regina Yole Guerra - CRB-8/4208 | Anderson de Santana - CRB-8/6658

Dourado Rodrigues da Silva, Anderson

Ore-genesis and evolution of the Pb-Zn-Ag-(Cu- Ba) deposits hosted by Perau Formation, Southern Ribeira Belt, Brazil / Anderson Dourado Rodrigues da Silva; orientador Frederico Meira Faleiros. -- São Paulo, 2019. 68 p.

Dissertação (Mestrado - Programa de Pós-Graduação em Mineralogia e Petrologia) -- Instituto de Geociências, Universidade de São Paulo, 2019.

1. Fluid Inclusions. 2. Sulfide Mineral Chemistry. 3. Sulfur Isotopes. I. Meira Faleiros, Frederico, orient. II. Título.

UNIVERSIDADE DE SÃO PAULO
INSTITUTO DE GEOCIÊNCIAS

Ore-genesis and evolution of the Pb-Zn-Ag-(Cu-Ba) deposits hosted by the Perau Formation, Southern Ribeira Belt, Brazil

ANDERSON DOURADO RODRIGUES DA SILVA

Orientador: Prof. Dr. Frederico Meira Faleiros

Dissertação de Mestrado

Nº 846

COMISSÃO JULGADORA

Dr. Frederico Meira Faleiros

Drª. Lena Virginia Soares Monteiro

Dr. Washington Barbosa Leite Junior

SÃO PAULO
2019

ACKNOWLEDGMENTS

To my wife, for all the support during these last two years, for being my safe haven and for always being available to be my first reviewer.

I would like to thank my family for all the good examples that each one of them has given me over the years, and especially for the support in the pursuit of constant personal and professional development.

I want to express my gratitude to my advisor, Prof. Dr. Frederico Meira Faleiros, for the example of dedication, instructions, and above all, for the commitment throughout the execution of this master's dissertation.

Thanks to all my friends from CPRM/SUREG-SP (Elizete, Angela, Mauricio, Vydia, Ivan, Francisco, Felipe, Ligia, Sergio, Luiz Gustavo, and Fabrizio) that somehow contributed in the execution of this master's dissertation.

Thanks to my friends Jairo, Caio, Rafael, and Marco for their friendship, corrections, and especially for the logistical support in my countless trips to São Paulo.

RESUMO

Os depósitos de Pb-Zn-Ag-(Cu-Ba) de Canoas e do Perau localizam-se na porção sudeste do estado do Paraná, próximo à divisa com o estado de São Paulo, em região denominada de Vale do Ribeira. Esses depósitos são classificados, por diversos autores, como do tipo Sedex (sedimentar exalativo). A região do Vale do Ribeira apresenta registros da exploração de chumbo desde meados da década de 1950, tendo sido responsável por toda a produção brasileira naquele período. Este trabalho investigou os depósitos de Canoas e Perau por meio de (1) compilação e integração de dados de estudos metalogenéticos prévios, (2) coleta de novos dados geológicos em campo, (3) redescrição de furos de sondagem realizados pela CPRM na década de 1980, (4) análises químicas minerais e de isótopos de enxofre em sulfetos de horizontes mineralizados, e (5) estudos de inclusões fluidas em quartzo de amostras de horizontes mineralizados. O quadro geológico dos depósitos de Canoas e Perau é dominado por uma sucessão metavulcano-sedimentar de idade Calimiana (ca. 1475-1490 Ma), denominada de Formação Perau, que integra o Terreno Apiaí da Faixa Ribeira Meridional, localizada na porção central da Província Mantiqueira. O minério dos depósitos do Perau e de Canoas é caracterizado por níveis de sulfeto maciço e disseminado constituídos predominantemente pela associação galena-esfalerita-calcopirita-pirita, com quantidades variáveis de barita ao longo de horizonte mineralizado denominado de Horizonte Perau. Os níveis sulfetados estão intercalados em pacote de rochas calciossilicáticas da unidade de xistos da Formação Perau, que foram submetidos à deformação e metamorfismo em fácies xisto verde alto a anfibolito no Neoproterozoico (615-570 Ma), durante a orogenia Brasiliana/Pan africana.

Dados de isótopos de enxofre, obtidos para os depósitos de Canoas e do Perau (+1.2 a +13.16 ‰ e -1.88 a +3.25‰, respectivamente) apresentam valores semelhantes a outros depósitos do tipo SEDEX de idade Proterozoica, com a fonte do enxofre sendo dominada por água do mar reduzida a partir de mecanismos de BSR (redução biogênica de sulfato) e TSR (redução termoquímica de sulfato). Análises de química mineral em esfalerita revelam diferenças no conteúdo de Fe entre os minérios ricos em barita (1.22% em peso) e sílica (7.24% em peso), indicando diferenças na temperatura de precipitação da esfalerita entre esses dois tipos de minérios. Dados microtermométricos obtidos sugerem a atuação de fluidos metamórficos caracterizados por inclusões fluidas primárias com Th intermediária (255 – 401 °C) e baixa salinidade (0,45 a 2,35% em

peso de NaCl equiv.) e por inclusões aquosas secundárias com Th (108 – 203°C) e valores de salinidade intermediárias a altas (6,44 a 25,33% em peso de NaCl equiv.). Os fluidos caracterizados representam os sistemas H2O-NaCl-MgCl2-CO2 para as inclusões primárias e H2O-NaCl-CaCl2 para as inclusões aquosas secundárias. Ambos os sistemas, constituídos por complexos cloretados, atuaram na remobilização e reconcentração das mineralizações primárias durante a deformação e o metamorfismo no Neoproterozoico.

Palavras-chave: Formação Perau; Depósitos Sedex; Horizonte Perau; Química Mineral; Isótopos de Enxofre; Inclusões Fluidas

ABSTRACT

The Canoas and Perau Pb-Zn-Ag- (Cu-Ba) deposits are located in the southeastern portion of the state of Paraná, near the border with the state of São Paulo, in a region called Vale do Ribeira. Various authors classify these as Sedex (sedimentary exhalative). The Ribeira Valley region has records of lead exploitation since the mid-1950s, having been responsible for all Brazilian production in that period. This work investigated Canoas and Perau deposits by (1) compiling and integrating data from previous metallogenetic studies, (2) collecting new geological data in the field, (3) redescription of drill holes conducted by CPRM in the 1980s, (4) analyzes of sulfide mineral chemistry and sulfur isotopes in sulfides of the mineralized horizon, and (5) fluid inclusion studies in quartz of samples from the mineralized horizon. A Calymmian metavolcano-sedimentary succession (ca. 1475-1490 Ma), called the Perau Formation, dominates the geological framework of the Canoas and Perau deposits, which forms part of the Apiaí Terrane of the Southern Ribeira Belt, located in the central portion of the Mantiqueira Province. The Canoas and Perau deposits ore is characterized by massive and widespread sulfide levels consisting predominantly of the galena-sphalerite-chalcopyrite-pyrite association, with varying amounts of barite along the mineralized horizon called "Horizonte Perau". The sulfide levels are intercalated in a package of calc-silicate rocks from the Perau Formation schist unit, which underwent deformation and metamorphism in high greenschist to amphibolite facies in the Neoproterozoic (615-570 Ma) during the Brasiliano / Pan African orogeny.

Sulfur isotope data obtained for Canoas and Perau deposits (+1.2 to +13.16 ‰ and -1.88 to + 3.25 ‰, respectively) show values similar to other Proterozoic-age SEDEX deposits with the sulfur source being dominated by seawater reduced by mechanisms of BSR (biogenic sulfate reduction) and TSR (thermochemical sulfate reduction). Analyzes of sphalerite mineral chemistry reveal differences in Fe content between barite (avg. 1.22 wt%) and silica (avg. 7.24 wt%) rich ores, indicating differences in sphalerite precipitation temperature between these two types of ore. Microthermometric data suggest the performance of metamorphic fluids characterized by primary fluid inclusions with intermediate Th (255 - 401 ° C) and low salinity (0.45 to 2.35% by weight of NaCl equiv.) and, by secondary aqueous inclusions with Th (108 - 203 ° C) and intermediate to high salinity values (6.44 to 25.33 wt% equiv. NaCl). The described fluids represent the H2O-NaCl-MgCl2-CO2 systems for the primary

inclusions and H2O-NaCl-CaCl2 for the secondary aqueous inclusions. Both systems consist of chloride complexes, worked on the remobilization and, the reconcentration of primary mineralization during deformation and metamorphism in the Neoproterozoic.

Keywords: Perau Formation; Sedex Deposits; Horizonte Perau, Sulfur Isotopes; Mineral Chemistry; Fluid Inclusions

TABLE OF CONTENTS

LIST OF FIGURES

LIST OF TABLES

1. INTRODUCTION

The southern Ribeira Belt is nationally recognized as an important Metallogenetic Province, being responsible for all of Brazil's lead production during the first half of the twentieth century. Several projects with the objective on the evaluation of the mineral potential of the southern Ribeira Belt have been carried out since the 1970s, highlighting regional geochemical recognition developed by the Geological Survey of Brazil/CPRM (Addas and Vinha, 1975, Morgental *et al*., 1975a, b; Morgental *et al*. 1978). These works have indicated significant anomalies of copper, lead, and zinc and guided detailed research focusing on prospecting for gold and associated sulfides. The first discoveries of mineral resources in the Perau Formation date back from the middle of the 1920s, when copper occurrences were identified in a level of dolomites, being explored as galleries during the World War II (Souza, 1972). The advance of mineral exploration in the region of the copper galleries culminated in the discovery of a level, stratigraphically above copper mineralization, containing significant contents of Pb-Zn. According to Daitx (1996), mining activities in the Perau region began in 1974 through open-pit mining. In the Canoas area, research work began in 1976, resulting in the discovery of similar mineralization to that found in the Perau region.

During the 1980s, CPRM implemented, through partnerships, two significant projects in the southern Ribeira belt. These projects had as a goal the homogenization of the geological data of the region and the detailed study of two mineralized areas in Pb-Zn (hosted by Lajeado Group and Perau Formation) to establish parameters about the characteristics and the differences between these two mineralizations, known as Perau-type and Panelas-type (Fleischer *et al*., 1976). The "Anta Gorda Project" (MMAJ-JICA, 1981, 1982, 1983, 1984; Daitx *et al*., 1983; Daitx, 1984) was developed by CPRM, together with Japan International Cooperation Agency/JICA and Metal Mining Agency of Japan/MMAJ. The "Projeto Integração e Detalhe Geológico do Vale do Ribeira" (Silva *et al*., 1981) executed through a cooperation agreement between CPRM and the National Department of Mineral Production/DNPM, known today as the National Mining Agency/ANM.

During the 1990s, the work of Daitx (1996) on the origin and evolution of the Perau and Canoas deposits made essential advances in understanding the exhalative sedimentary origin of these deposits. Recently, Fedalto (2018) studied the role of deformation and metamorphism in changing the original conditions of mineralized

levels through the development of textures and structures observed in the outcropping mineralization of the Perau area.

This work was based on a multi-technique approach that included field geology, petrography, ore geochemistry, mineral chemistry, stable isotopes, and microthermometry of fluid inclusions. The achieved results aided in determining the possibility of multistage genesis, lithotypes, mineral assemblages, and fluid evolution during the sedimentary exhalative origin and the post remobilizations of the Pb-Zn-Ag (Cu-Ba) mineralization.

1.1. Location and Access

The study area (Fig. 1) is located in the state of Paraná, between the municipalities of Tunas do Paraná and Adrianópolis, nearby to the border with the state of São Paulo. The access from the São Paulo city to Adrianópolis city is made by the Raposo Tavares (SP-270) and SP-127 highways until the bridge that crosses the Ribeira River connecting the towns of Ribeira, state of São Paulo, to the city of Adrianópolis in the state of Paraná.

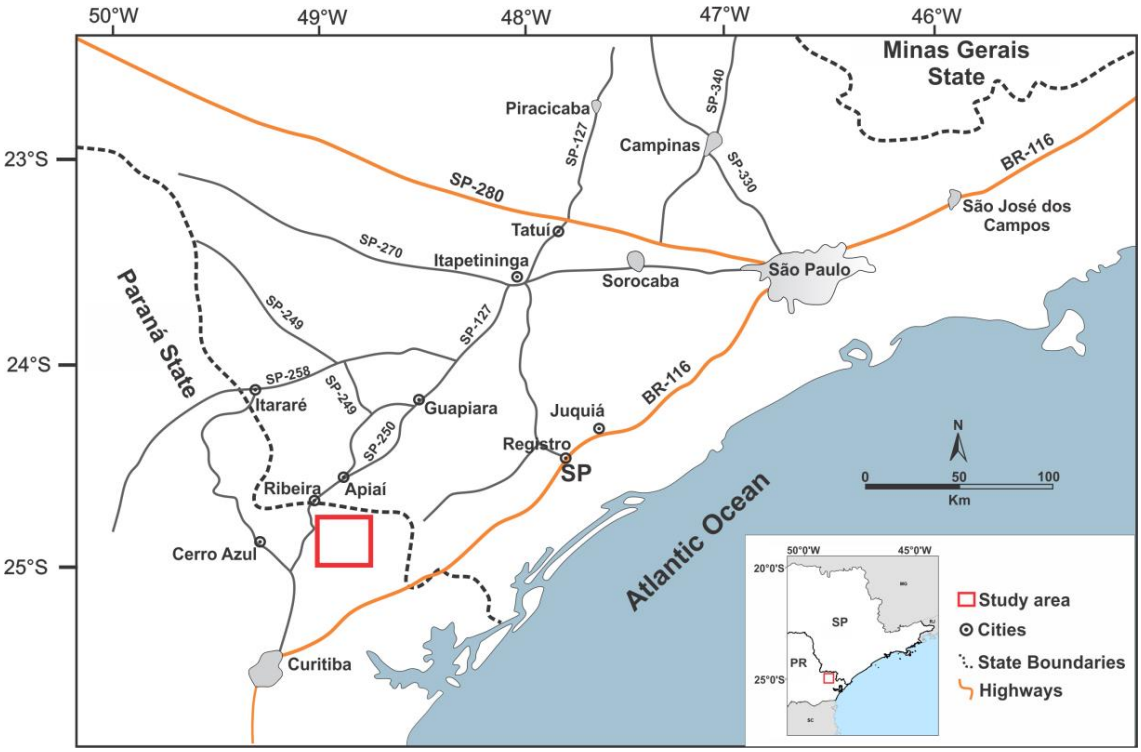

Fig. 1. Location and access to the study area from the cities of São Paulo and Curitiba, states of São Paulo and Paraná, respectively.

1.2 Research Aims

The objective of this master's dissertation is based on the determination of the process related to the formation of polymetallic (Pb-Zn-Ag-Cu-Ba) mineralizations hosted by the Perau Formation and post-ore remobilization due to deformation and metamorphism.

1.3 Questions to Answer

This master's dissertation has six main issues, which motivated its conduction and seeks to be used as a guideline to answer the following questions:

(1) Is the sulfides compositions in the Perau and Canoas deposits similar or distinct and what is the relevance of that for ore genesis?

(2) Is the chemical composition of sulfides from the Canoas and Perau deposits recording primary genesis or metamorphic remobilization processes?

(3) What are the sources of sulfur in the Perau and Canoas deposits?

(4) Are the sulfur isotope conditions of Perau and Canoas similar?

(5) Are primary mineralizing fluids preserved as fluid inclusions in ore samples?

(6) What is the role of the metamorphic fluids on the sulfide mineralization, are there capable to remobilize/concentrate metal contents?

2. MATERIAL AND METHODS

The project started with the organization of a georeferenced base containing all the available information for the region, including data from previous projects and the integration and preliminary interpretation of geological, geophysical, geochemical and remote sensing bases. Subsequently, fieldwork activities, petrographic, lithogeochemical analyses, isotopic determinations, and fluid inclusions analyses were performed.

2.1 Literature Review

The literature review was carried out throughout the development of the project, with a focus on understanding the current state of the geological knowledge of the Southern Ribeira Belt, especially its polymetallic mineralizations. Geological mapping products, geophysical surveys, remote sensing images, structural and geochemical data from previous projects were compiled and analyzed.

2.2 Fieldwork

Fieldwork had as objective the description of the remaining outcropping mineralizations, especially in the areas of Perau and Canoas. Regional profiles throughout these areas were executed to understand the relationships of the mineralized units in the regional context. In the field studies, concentrated in the mineralized areas, 47 outcrops were described, and 45 samples were collected. In addition, in a study carried out in the Araraquara lithotheque (LIAR-CPRM), the samples of six drill holes, located in the southwest area of the Perau Mine, executed in the Anta Gorda project through partnership between the CPRM, the MMAJ and the JICA (1981, 1982, 1983, 1984) were described and sampled.

2.3 Petrography

Petrographic analyses were concentrated on samples of the mineralized horizon and their host rocks, which were collected in the field and from drill holes of the Anta Gorda project.

A total of 61 thin-polished sections were made in the laminating laboratories of the CPRM (at the Araraquara lithotheque and the Regional Superintendence of

Salvador) and were described in an Olympus BX51 microscope in the CPRM petrography laboratories, in the offices of Brasília and São Paulo.

2.4 Lithogeochemistry

Samples of the mineralized zones of the Canoas deposit were sent for analysis at SGS Geosol Laboratórios Ltda. Determinations of the concentrations of the major elements were obtained employing X-ray fluorescence (XRF). For determination of the trace elements, total digestion of the samples was initially performed by acid etching (nitric, hydrochloric, hydrofluoric and perchloric acids) or by melting with lithium metaborate. Subsequently, the samples were analyzed by Inductively Coupled Plasma Spectrometry (ICP-MS) and Inductively Coupled Plasma Emission Spectrometry (ICP-OES). The concentrations of Au, Pt, and Pd elements in ore samples were obtained by the fire assay method with ICP-OES reading and the Ag element by Atomic Absorption Spectrometry (ASA). A total of 10 rock samples were analyzed, aiming to determine metal contents, as well as the compositional variation of elements of interest in the mineralized zones and respective host rocks.

2.5 Mineral Chemistry

A total of six thin-polished sections were analyzed in Electron Probe Microanalyser (EPMA) at the of the Federal University of Goias (Brazil), using a JEOL model JXA-8230 microprober, operating with an acceleration voltage of 15 kV and 20 nA to mafic carbonates and minerals and 20 kV and 40 nA to sulfides. The analysis time varied from 10 to 30 seconds, according to the expected abundance of each element in the mineral.

2.6 Isotopic analysis

Sulfur isotope analyses of 13 samples from the polymetallic mineralizations of Canoas Mine and in the samples of the drill holes of Anta Gorda Project, were carried out in the Stable Isotope Laboratory at the University of Brasília (Brazil). For sulfur analysis, SO_2 was produced by combustion of about 0.5 mg of pyrite, chalcopyrite, galena, and sphalerite loaded into tin capsules reacting at 1080 °C. The combusted gases were carried in a He stream and reduced by contact with high-purity copper wires, and

the SO_2 was separated by gas chromatography. Analyses were conducted by the EA-IRMS (Elemental Analysis e Isotope Ratio Mass Spectrometry), using a Flash Elemental Analyzer and ThermoFisher MAT 253 mass spectrometer. Uncertainties are estimated at 0.2‰.

2.7 Fluid inclusion studies

Fluid inclusion petrography and microthermometric analyses were accomplished on 8 doubly-polished sections (100 μm thick) of the polymetallic mineralizations of Canoas Mine and in samples of drill holes of the Anta Gorda Project (AG-01, AG-02, AG-04 e AG-05). Microthermetric analysis were performed at the Fluid Inclusion Laboratory, Institute of Geoscience, University of São Paulo, using a Linkam THMSG600 stage with a T94 controller and digital positioning system, coupled to an Olympus BX51 binocular microscope, and in the Fluid Inclusion Laboratory of the Geological Survey of Brazil, using a Linkam THMSG 600 stage with a LTS420 controller. The stages were calibrated with synthectic fluid inclusion (CSCO2) standards for high and low temperatures.

The estimated precision is ± 0.1 ºC for temperatures of CO_2 homogenization ($ThCO_2$), and CO_2 melting ($TmCO_2$), ± 0.2 ºC for clathrate dissociation (Td_{Cl}) and ice melting (Tm_{Ice}), ± 1 ºC for eutectic melting of aqueous-carbonic and aqueous inclusions (T_E) and ± 2 ºC for total homogenization (Th). Physico-chemical properties of trapped fluids and isochores were calculated with the computer software packages FLUIDS and CLATHRATES (Bakker, 1997, 2003).

3. TECTONIC SETTINGS

The works in the Ribeira Belt (defined by Hasui *et al*., 1976) are usually initiated with the location of the study area within the Mantiqueira Province (Fig. 2), south and southeast portion of the South American Platform (Almeida, 1967; Almeida *et al*. 1977, 1981). A remarkable and undeniable feature of this Province is the division into elongated, anastomosed bands bounded by NE-directing transcurrent shear zones and prevailing Ediacaran to Cambrian movements. The Ribeira Belt constitutes the central portion of the Mantiqueira Province, with evident records of a transcurrent system of ductile-brittle character. In its southern part, consists of reworked tectonic terrains of distinct origin, constituted by Archaean to Paleoproterozoic basement rocks, Mesoproterozoic and Neoproterozoic volcano-sedimentary sequences (Paranaguá, Luís Alves, Costeiro, Curitiba, Embu, and Apiaí terrains), and different types of granites that intruded the basement and supracrustal rocks (e.g., Faleiros, 2008, Faleiros *et al*., 2010, 2011, 2016).

The Apiaí Terrane, one of the major domains of the Southern Ribeira Belt, is characterized by a sequence of supracrustal rocks submitted to metamorphism in greenschist to amphibolite facies conditions. Initially, the sedimentary rocks from this terrane were attributed to the Açungui Group and later redefined as the Açungui Supergroup (Campanha, 1991; Campanha and Sadowski, 1999). According to Campanha and Faleiros (2005), based on geological, petrological and geochronological data, the Apiaí Terrane consists of a combination of distinct tectono-stratigraphic terranes (sensu Howell, 1995) with Mesoproterozoic to Neoproterozoic ages accretionated during the Neoproterozoic, with the later stages of accretion defined by a dextral transcurrent system and an oblique continental collision. It is composed of rocks with Calymmian ages (ca. 1450-1500 Ma: Votuverava Group- Perau, Rubuquara. Nhunguara, Piririca and Ribeirão das Pedras Formations-, Serra das Andorinhas Sequence and Água Clara Formation), Stenian-Tonian (ca. 1200-880 Ma: Lajeado Group and part of the Itaioca Group) and Ediacaran (630-580 Ma: part of the Itaioca Group and Iporanga Formation), added during the Brasiliano-Pan-African Orogeny (Campanha and Faleiros, 2005; Faleiros, 2008; Campanha et al., 2015, 2016). The basement rocks consist of Paleoproterozoic migmatitic and mylonitic orthogneisses (ca. 1750-1800 Ma) (Cury *et al*., 2002; Pazeres Filho, 2005; Ribeiro, 2006), mainly in the nucleus of some restricted antiforms.

The Perau Formation hosts the Perau and Canoas Pb-Zn-Ag (Ba-Cu) deposits, which are inserted within the Votuverava Group in the Apiaí Terrane.

3.1 Perau Formation

The rocks that comprise the Perau Formation were initially studied by Piekarz (1981) and Takahashi *et al*. (1981), but this denomination was firstly attributed in the work of Fritzson Jr. *et al*. (1982), which defined it as the basal unit of the Setuva Group. According to the authors, the formation consists of quartzite, schist, metabasite, metavolcanics rocks, metavolcanoclastic rocks, and iron formations. Soares (1987) infer the Perau Formation was deposited in an environment of stretched and rifted passive continental margin, in which coastal, platform, and basinal environments were developed, with the formation of oceanic crust, that would have evolved to a back-arc basin.

Daitx (1996) describes that the sedimentation of the carbonate rocks occurred under platform conditions along tectonic sub-basins formed in a rift-type extensional regime, with high thermal flow probably related to magmatic activities. The author indicates the elongated shape in the NE-SW direction, narrow and partially segmented, to the sedimentation environment. According to the author, the Perau Formation corresponds to a volcano-sedimentary sequence of the oceanic bottom, with the generation of SEDEX (sedimentary-exhalative) type deposits, that was submitted to metamorphism in the greenschist to lower amphibolite facies conditions. U-Pb data, obtained by Basei *et al*. (2003) in zircon of amphibolite rocks from the Perau Formation provide an age of 1484 ± 16 Ma that are close to those obtained in other Formations of the Votuverava Group Formation (Campanha *et al.*, 2008, 1439 ± 19 Ma).

The data obtained by Basei *et al*. (2003) are compatible with the age of the mineralization, 1380-1440 Ma in the Perau Formation, obtained by the Pb-Pb method in galena of the mineralized horizon (Tassinari *et al*., 1990; Daitx, 1996), which, according to the authors indicate the syngenetic origin of Pb-Zn-Ag-(Cu-Ba) mineralizations.

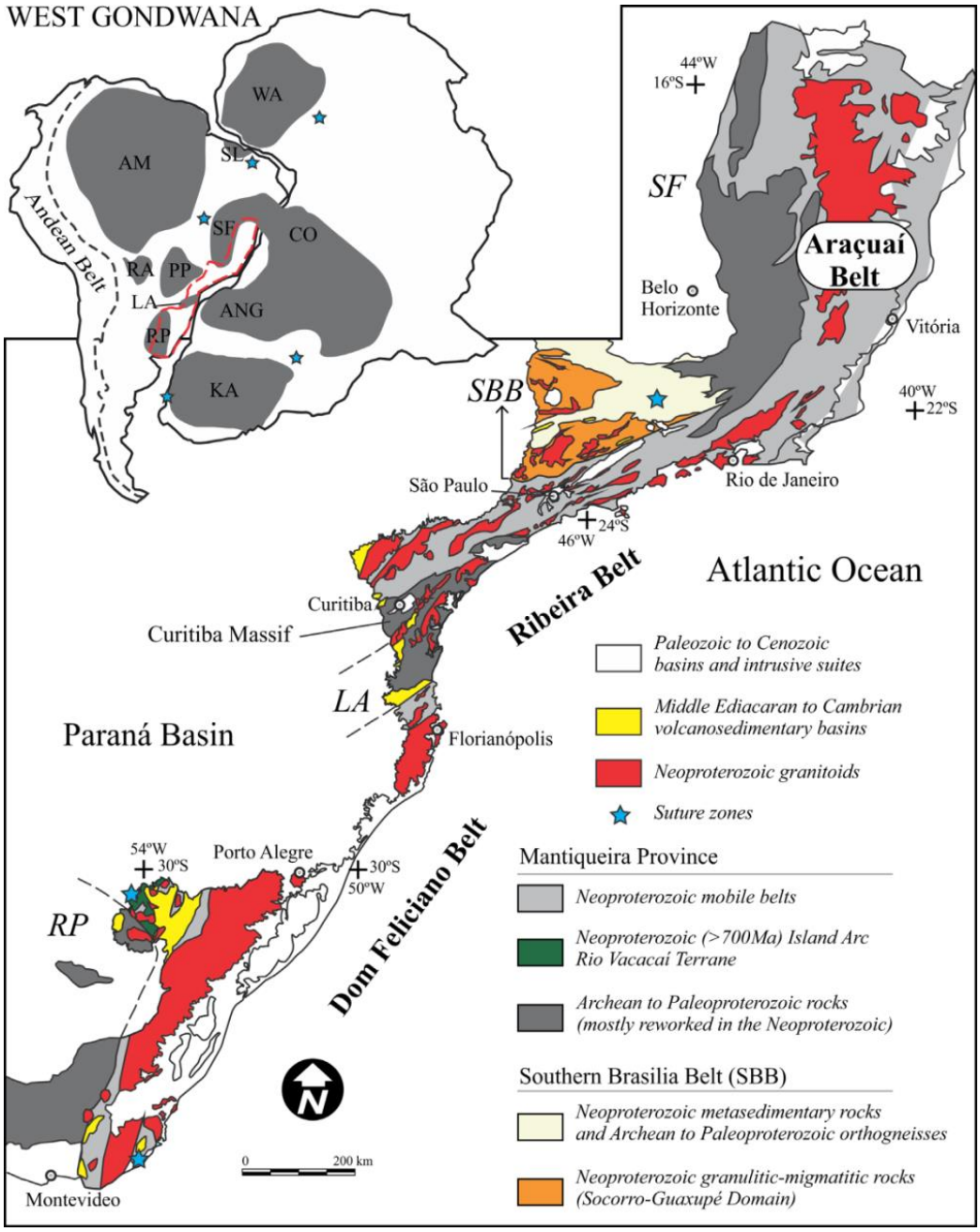

Fig. 2. Tectonic map and main geological units of the Mantiqueira Province: The inset shows the cratonic blocks of Western Gondwana. Abbreviations: AM, Amazonian Craton; ANG, Angola Block; CO, Congo Craton, KA, Kalahari Craton; KA, Kalahari Craton; LA, Luis Alves Craton; PP, Paranapanema Block; RA, Rio Apa Block; RP, Rio de La Plata Craton; SL, São Luis Craton; WA, West Africa Craton. Modified from Meira *et al*. (2015).

For Siga Jr. (2011), the Betara and Perau formations comprise two metavolcano-sedimentary sequences of Mesoproterozoic age, suggesting tectonic contacts with the Betara and Tigre nuclei. According to the author, those formations present stratigraphic correlation being composed, from the base to the top, by a quartzite basal succession with planar cross-stratification of low to medium angle, deposited in coastal environment; an intermediate succession of carbonate rocks associated with

metavolcanic rocks, which contains Pb, Zn, Ag and Cu anomalies; and a metapelitic succession at the top.

According to Faleiros *et al*. (2012), the Perau Formation is constituted, from the base to the top, by a quartzite unit, followed for the shale unit. In this unit, lenticular bodies of amphibolites and carbonaceous rocks with polymetallic mineralized zone occur. The author describes anticline and syncline folds in the Perau Formation, with subhorizontal SW-plunging axis oriented, which characterizes an anticline supported by the quartzite unit. The deformation of the schist unit is attributed to the NE-trending Ribeirão Grande Shear Zone.

CHAPTER 4 – FLUID INCLUSIONS, SULFUR ISOTOPES, AND SULFIDE MINERAL CHEMISTRY OF THE Pb-Zn-Ag-(Cu-Ba) DEPOSITS OF THE PERAU FORMATION, RIBEIRA MERIDIONAL BELT, PARANÁ.

Anderson Dourado Rodrigues da Silva[1,2]*, Frederico Meira Faleiros[3]
[1] Geological Survey of Brazil – CPRM; Brasília, DF. CEP: 70.297-400
[2] Programa de Pós-Graduação Geociências (Mineralogia e Petrologia), Instituto de Geociências, Universidade de São Paulo
[3] Departamento de Mineralogia e Geotectônica, Instituto de Geociências, Universidade de São Paulo, Rua do Lago, 562, 05508-080, São Paulo, SP, Brazil.
*corresponding author: e-mail address: anderson.rodrigues@cprm.gov.br

Abstract

The Pb-Zn-Ag-(Cu-Ba) deposits of the Perau Formation, located in the southern Ribeira Belt, in the central part of Mantiqueira Province, Brazil, were studied in detail in this work. Sulfur isotopic compositions of sulfide minerals are determined in the areas of Canoas and Perau deposits, geochemical investigations of sulfides from the mineralized calc-silicate rocks were carried out using electron probe micro-analysis (EPMA), and microthermometric studies were performed in quartz from the "Horizonte Perau." Sulfur isotopic data from 13 sulfide samples from Canoas and Perau deposits are presented. The S-isotopic compositions obtained (Perau deposit: -1.88 to +3.25‰, and Canoas mine: +1.2 to +13.16 ‰) are in the same range of other Proterozoic Sedex deposits with the source of sulfur been dominated by reduced seawater sulfate produced by BSR and TSR mechanisms. Sulfide mineral chemistry of sphalerite show differences in Fe content between barite and silica-rich ores, suggesting differences in the precipitation temperatures of these two types of ore. Fluid inclusion data show a population of three assemblages, one of primary fluid inclusions with intermediate Th (255 – 401°C) and low salinities (0.45 to 2.35 wt. NaCl equiv.), another of secondary carbonic inclusions with $ThCO_2$ (-57.6 to -56.6), indicating CO_2 is the dominant volatile, and another of secondary aqueous fluid inclusions with Th (108 – 203°C) and intermediate to high salinities (6.44 to 25.33 wt.% NaCl equiv.) which are interpreted as metamorphic. The studies suggest a H_2O-NaCl-$MgCl_2$-CO_2 fluid composition for primary and a H2O-NaCl-$CaCl_2$ fluid composition for secondary aqueous fluid inclusions. Both systems have the capacity of remobilization of the previous base metals mineralization. The interpretation of these data together adds new perspectives in the study of the evolution of the deposits hosted by Perau Formation.

Keywords: Perau Formation; Sedex; Sulfur sources; Fluid inclusion; Sulfide Mineral Chemistry; Metamorphism.

4.1. Introduction

The southern Ribeira Belt, in the Mantiqueira Province (Fig.3), is recognized as an important Metallogenetic Province, having been responsible for all of Brazil's lead

production during the first half of the twentieth century. Production of base metals started in the early 1920s in the Lajeado Group and Cupper gallery (Figs. 3 and 4). For the Pb-Zn-Ag (Cu-Ba) mineralizations hosted by Perau Formation, the production started at the Perau area in 1974. In 1976, exploration programs began in the Canoas area (Daitx, 1996). Despite the economic importance of these mineralizations, there is a lack in the understanding of the conditions and differences in the ore genesis of deposits hosted by the Perau Formation and Lajeado Group (Fig. 3; Fleischer, 1976; Barbour *et al*. 1990; Daitx, 1996). The syngenetic origin of Perau Formation mineralizations has been admitted for several authors, which classify these deposits as sedimentary exhalative (SEDEX) (e.g., Barbour and Oliveira, 1979; Daitx, 1996; Dardenne and Schobbenhaus, 2001). The SEDEX deposits are described as sedimentary rock-hosted sulfide-dominated Pb-Zn ore bodies with sphalerite and galena as the principal ore minerals (Goodfellow *et al*., 1993; Lydon, 1996; Large *et al*., 2004; Goodfellow and Lydon. 2007), formed in structurally controlled sedimentary basis through submarine venting of hydrothermal fluids. Studies about post-ore genesis modifications, in Perau Formation, due deformation and metamorphism are scarce, with only a few published works (Fedalto, 2018; Silva *et al.*, 2019).

In this paper, we use a multi-technique approach that include field geology, petrography, structural analyses, ore geochemistry, mineral chemistry, stable isotopes and, microthermometry of fluid inclusions. The achieved results aided to determine the possibility of a multistage genesis, the main controls, lithotypes, mineral assemblages, and fluid evolution during the primary origin and the post remobilizations of the Pb-Zn-Ag (Cu-Ba) mineralization.

4.2. Geotectonic Settings

The study area is located in the Mantiqueira Province, a branched system of orogens placed in the south and southeast regions of Brazil (Almeida *et al*., 1977, 1981; Brito Neves et al., 1999). The Mantiqueira Province comprises the Araçuaí, Ribeira, southern Brasilia, Dom Feliciano, and São Gabriel belts (Heilbron *et al*., 2003). It is the result of the amalgamation of paleocontinent Western Gondwana during the Neoproterozoic Braziliano-Pan African orogeny (e.g. Brito Neves *et al*. , 1999; Campanha and Sadowski, 1999; Heilbron and Machado, 2003; Heilbron *et al*. , 2000a, b; Heilbron, *et al.*, 2008; Campanha and Faleiros, 2005). The Pb-Zn-Ag (Ba-Cu) mineralizations hosted by the Perau Formation are inserted within the Apiaí Terrane,

located in the southern portion of the Ribeira belt (Campanha and Sadowski, 1999) (Fig. 3).

The Ribeira Belt consists of a complex collisional orogeny related to oblique collisions between Paranapanema, São Francisco, and Congo cratons during the consolidation of the Western Gondwana supercontinent (Brito Neves *et al.,* 1999; Campanha and Brito Neves, 2004; Fuck *et al.,* 2008). Its southern portion consists of reworked tectonic terranes of distinct origins (Paranaguá, Luís Alves, Costeiro, Curitiba, Embu, and Apiaí terrains).

The Apiaí Terrane, characterized by a succession of supracrustal rocks submitted to metamorphism in greenschist to amphibolite facies conditions, is located to the north of the Lancinha Shear Zone (Fig. 3). Originally, these rocks were attributed to the Açungui Group and later were redefined as the Açungui Supergroup (Campanha, 1991; Campanha and Sadowski, 1999).

According to Campanha and Faleiros (2005), based on geochronological data, the Apiaí Terrane consists of a combination of distinct tectonic-metamorphosed terranes with Mesoproterozoic to Neoproterozoic ages accretionated during Neoproterozoic, with the later stages of accretion being characterized by a dextral transcurrent system and an oblique continental collision. It is composed of rocks of Calymmian (ca. 1450-1500 Ma: Group Votuverava, Perau Formation, Serra das Andorinhas Sequence and Água Clara Formation), Stenian-Tonian (ca 910-1030 Ma:. Itaiacoca part of the Group) and Ediacaran ages (ca 630-580 Ma: Iporanga Formation, and Lajeado Group), added during the Brasiliano-Pan-African Orogeny (Campanha and Faleiros, 2005; Faleiros, 2008). Basement rocks consist of orthogneisses migmatites and Statherian mylonites (ca. 1750-1800 Ma.) (Cury *et al*., 2002; Prazeres Filho, 2005; Ribeiro, 2006), outcropping mainly in the nucleus of some restricted to antiform structures.

The Votuverava Group, originally defined as a Formation (Bigarella and Salamuni, 1958), is limited to the south by the Lancinha Fault and to the north by the Figueira and Ribeira shear zones (Fig. 3). In its current stage, the Votuverava Group includes the Perau, Rubuquara. Nhunguara, Piririca and Ribeirão das Pedras Formations (Piekarz, 1981; Takahashi *et al*., 1981; Campos Neto, 1983; Perrota, 1996, Campanha and Sadowski, 1999) and other two undivided units (Faleiros et al., 2010, 2012; Faleiros and Pavan, 2013).

SHRIMP U-Pb data, obtained for Basei *et al.* (2008), of detrital zircon grains from phyllites of the Votuverava Group, indicated age peaks at ca. 3200–2800, 2400,

2200–1900 and 1750 Ma, placing, according to the authors, the possible sedimentation age in the late Paleoproterozoic. U-Pb dating on zircon from metabasic rocks that occur concordantly intercalated with the Votuverava Group rocks yielded concordant ages of 1439 ± 19 Ma (Votuverava Sequence, Campanha *et al*., 2008) and 1484 ± 16 Ma (Perau Formation, Basei *et al*., 2003). Recently, Campanha *et al.* (2015) obtained SHRIMP U–Pb ages of 1488 ± 4 Ma in metabasic rocks of the Rubuquara Formation These U-Pb zircon ages are interpreted for the authors as the minimum ages of the Votuverava Group sedimentation.

Several authors attributed a back-arc basin as the depositional environment of the Votuverava Group (Soares, 1987; Maniese, 1997). More recent, Campanha *et al.* (2015) used geological, geochemical, and geochronological data to suggest the existence of extensive 1490Ma oceanic back-arc basin magmatism related to the formation of metabasic rocks of the Votuverava Group.

The Votuverava Group shows evidence of Barrovian-type metamorphism in the metapelites ranging from the biotite zone grade to the kyanite zone (Faleiros *et al*., 2010; Yogi, *et al*., 2019). According to Yogi et al. (2019), the peak of metamorphism assemblage (kyanite zone), obtained with phase equilibria modeling, indicate conditions of 660°C and 7.6 kbar and posterior decompression on the order of 2-3 kbar To the authors, the contact between the orthogneisses of Tigre Nuclei and the quartzites of the Perau Formation (Fig. 3) record predominance of simple shear zone ductile deformation under greenschist to low amphibolite facies. ^{40}Ar-^{39}Ar obtained for Yogi *et al*. (2019) in hornblenda of amphibolite indicate cooling ages of 602.6 ± 6.9 Ma (Ediacaran) and ~720 Ma (Tonian-Cryogenian). The older cooling ages are interpreted, by authors, to be related to regional metamorphism resulted from the amalgamation of the Apiaí and Embu Terrains in around 800 Ma.

The Perau Formation corresponds to a metavolcano-sedimentary sequence of Mesoproterozoic age, in tectonic contact with the Tigre Nuclei, characteristic of a succession of oceanic bottom (Daitx, 1996; Siga, Jr., 2011). According to Faleiros *et al. (2012) is* constituted, from the base to the top, by a quartzite unit superimpose by a schist unit. The schists unit has lenticular bodies of amphibolites and calc-silicate rocks where the Pb-Zn-Ag-(Cu-Ba) mineralized zone occurs. The author describes anticline and syncline folds in the Perau Formation, with the axis oriented in the NE direction and low angle dip for SW, which characterizes an anticline supported by the quartzite unit. The deformation of the part of the schist unit is attributed, by the authors, to the

Ribeirão Grande Shear Zone with NE direction. The age of the mineralized calc-silicate rocks obtained by the Pb-Pb method in galena (Tassinari *et al*., 1990; Daitx, 1996) yielded ages of 1380-1440 Ma in the Perau Perau Formation, which, according to the authors, indicate the syngenetic origin of Pb-Zn-Ag mineralizations. The description of the main characteristic of the mineralized calc-silicate rocks are presented in the next section.

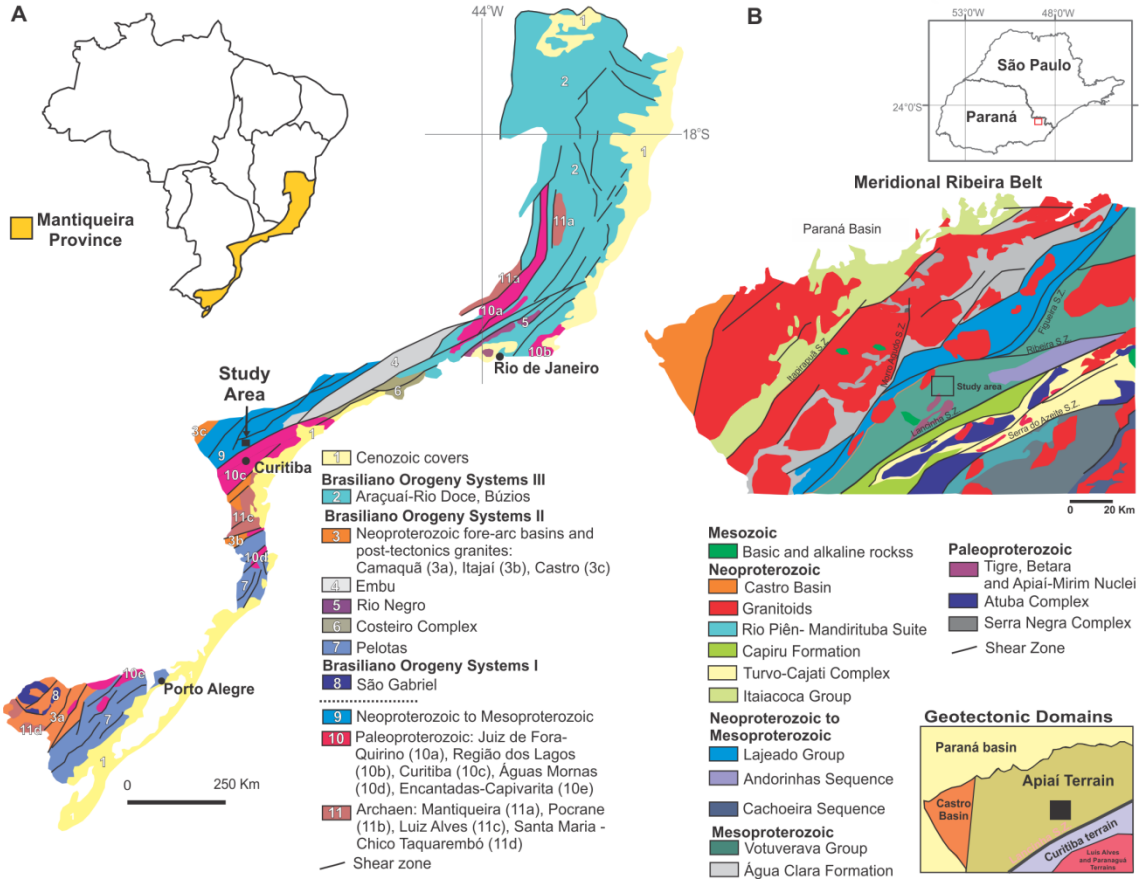

Fig. 3. (a) Location of the study area in the context of Mantiqueira Province, adapted from Delgado *et al*. (2003); (b) and in the context of Ribeira Meridional Belt, modified from Rodrigues *et al*. (2011).

4.2.1 Mineralizations of Pb-Zn-Ag (Ba-Cu) associated with Perau Formation

The first descriptions of the Pb-Zn-Ag (Ba-Cu) mineralization of the Perau Formation were initially performed by Baubour *et al*. (1979). These authors attribute to the deposit of the Perau mine exhaling sedimentary origin, according to criteria defined by Hutchinson (1979). Silva *et al*. (1982) describe the mineralizations as consisting of Pb, Zn, Ag, and Fe sulfides concordant with the host calc-silicate rocks and spatially related to magnetic banded iron formations. From the characteristics of the mineralized zone and associated iron formation, the authors inferred an exhalative system that was

the main supplier of metals related to the migration of metal-rich brines from upwelling areas to the banks of the basin.

The work developed in partnership with MMAJ / JICA (MMAJ-JICA, 1982) describes the characteristics of the mineralized horizon, designated by the authors as "the Perau Horizon" which occurs in association with lenses of calc-silicate rocks located in the basal portion of the lenses of carbonate rocks of the unit of schists. The authors describe the Perau Horizon as composed from top to bottom by a layer of graphite-mica-schist, the polymetallic mineralized zone (containing Pb-Zn-Ag-Cu sulfides), a layer of barite and a layer of magnetite enriched shale, considered as a guide layer for mineralization. The authors considered the deposit to be stratiform with general NE-SW direction, with vertical and lateral mineralogical zoning, whose geometry is influenced by the tectonic processes, characterizing an "S" shape attributed to the presence of folds. Daitx (1996) describes the mineralized zone as being marked by the alternation of layers rich in sulfide and the host rock. The ore minerals include galena, pyrite, sphalerite, and chalcopyrite, in addition to Ag-bearing phases, with quartz, calcite, and barite as gangue minerals.

In the area of the Perau mine, Daitx (1996) characterizes three main types of ore: copper, located below the graphite-mica schist layer, consisting mostly of pyrite, chalcopyrite and oxidized Cu minerals, without significant lead contents; barite, with disseminated galena, compositional banding and high levels of lead; and massive sulfide, considered the most common type in the mine that, according to the author, does not present the typical characteristics of this deposit. In the Canoas Mine, the author described two lentiform ore bodies with N50E direction, with widths between 75 and 200 meters and an extension of 1 km or more, truncated by a vertical N65W-trending fault.

Daitx (1996) performed a sulfur isotopic analysis in sulfides of the mineralized rocks of the Canoas deposit. For the author, the low values of $\delta^{34}S$ obtained suggest the deposition of sulfides occured from hydrothermal fluid circulation with sulfur derivated from a mixture of sulfur of magmatic origin and sulfur from the inorganic reduction of seawater sulfate. According to the author, the values of $\delta^{34}S$ are similar to the pattern exhibited for massive volcanogenic deposits with Proteroizoc and Fanerozoic ages and a few Sedex deposits.

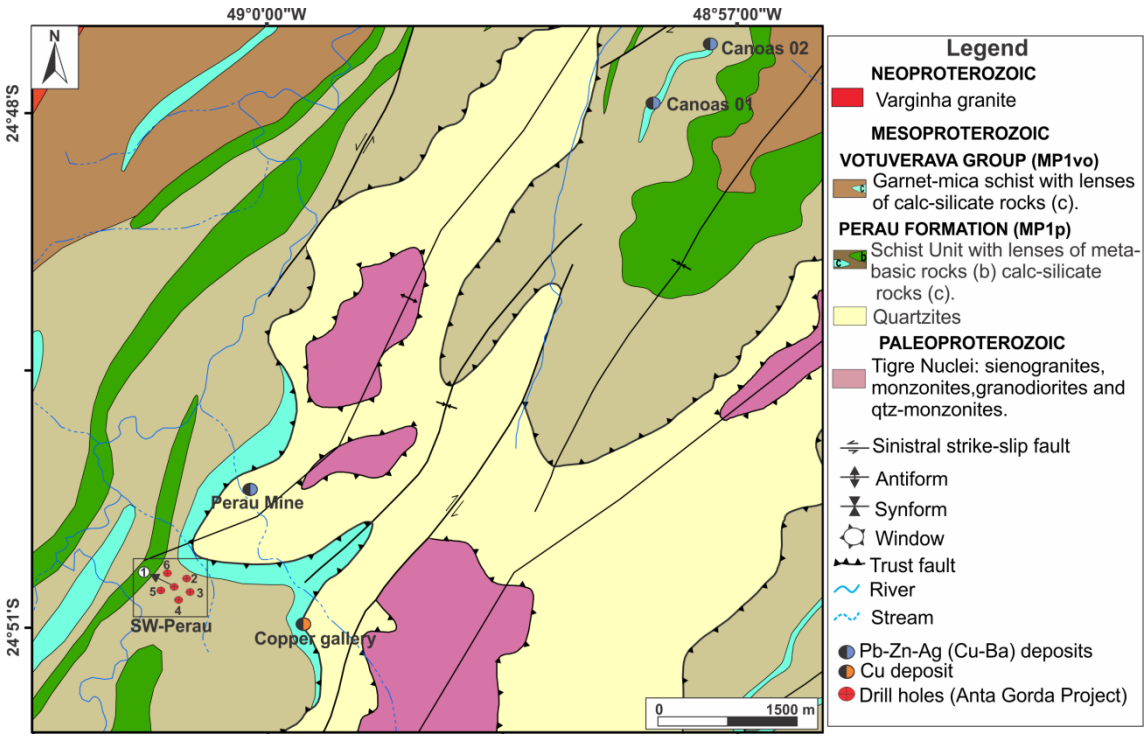

Fig. 4. Geological map of the Perau Formation (modified from Faleiros et al. 2010), with the location of the Perau and Canoas deposits.

4.3 Geology of Canoas and Perau Deposits

4.3.1 Perau Deposit Area

The polymetallic mineralization associated with the Perau mine area has been described in this work in two main sites (Copper Gallery and SW-Perau; Fig. 4) that have distinct characteristics. Major mining activities have taken place in the area of the Perau mine (Fig. 4), but nowadays the galleries where underground mining took place are inaccessible due to landslides.

4.3.1.1 Copper gallery

The copper prospect known as the copper gallery is composed of a Cu-rich level containing malachite, azurite, oxidized chalcopyrite, and Fe oxides, hosted by dolomitic marbles of the calc-silicate lens (Fig. 4). The mineralized level is concordant with the bedding (Fig. 5a, and b), presenting, on average, 20 centimeters of thickness in all the extension of the gallery (40 meters of length). The dolomitic marble hosting the mineralization has a massive appearance and white coloration with a sedimentary bedding (S0) parallel to a continuous schitosity (Sn) with average orientation of N40E/32NW. It is cut by a fracture system of average orientation of N80E/80SW. Along with the mineralized level, at the intersection with the sub-vertical fractures,

remobilization occurs in centimeter to decimetric scale (Fig. 5c). Brecciated levels with intense silicification locally occur (Fig. 5d).

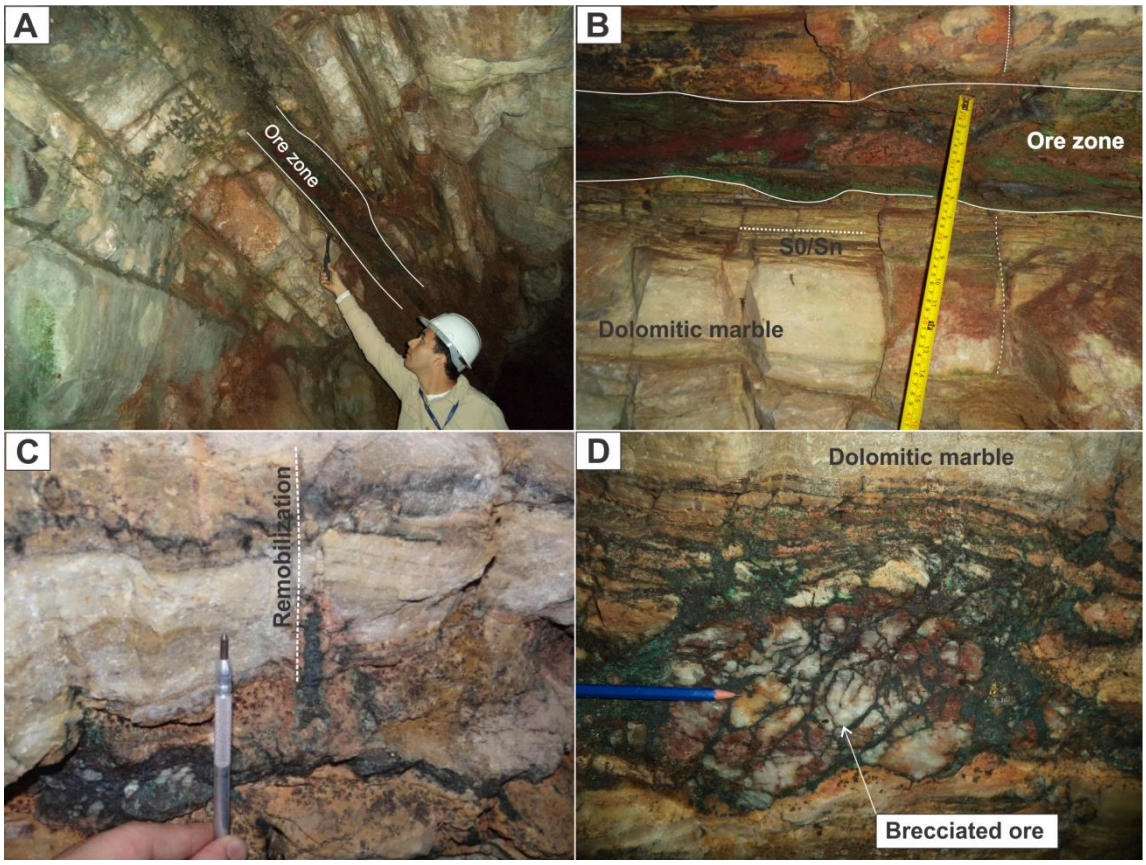

Fig. 5. General features of the ore in the Copper Gallery (Perau mine area). a, and b) Copper mineralized level concordant with dolomitic marble; c) remobilization by a sub-vertical fracture; d) Brecciated level associated with intense silicification.

Microscope analyses show that the dolomitic marble (Fig. 6a) is primarily composed of dolomite (85%) and quartz (15%), with minor biotite (<1%) (Fig. 6c). Incipient chalcopyrite grains occur disseminated at quartz levels in the impure dolomitic marble. Galena and sphalerite grains occur associated with fractures that cut the remobilized rocks. The brecciated ore (Fig 6b) is characterized by bands of medium-grained quartz with recrystallization microstructures and newly formed fine-grained quartz, along with opaque minerals (Fig. 6d).

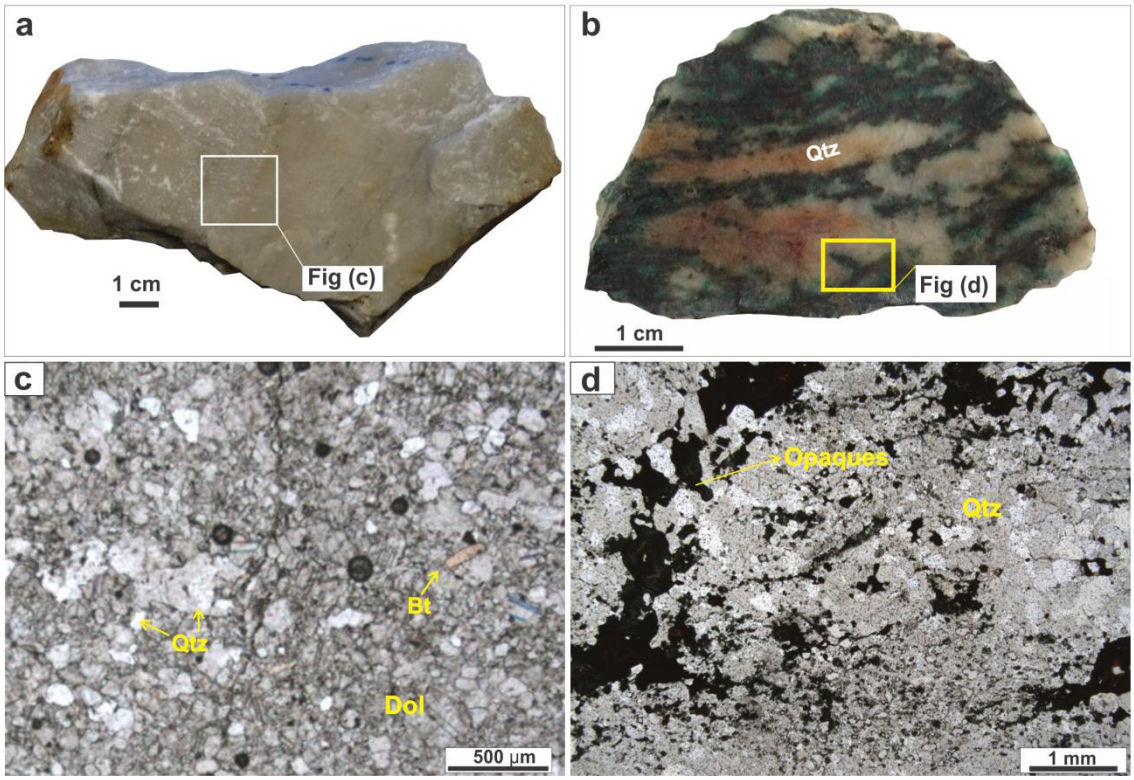

Fig. 6. Hand specimen (a, and b) and photomicrograph (c, and d) of host rock and brecciated level ore. (a) Dolomitic marble that hosts the Cu-rich level; (b) Brecciated level showing intense silicification related to weathering Cu-rich minerals; (c) Microscopic photomicrograph showing the composition of impure metadolomitic marble; (d) Brecciated level, under a microscope, showing the relation between silicification and opaque minerals. Qtz: quartz; Bt: biotite; Dol: dolomite.

4.3.1.2 SW Perau

Six drill holes executed southwest of the Perau mine (Fig. 4; MMAJ-JICA, 1983, 1984) confirmed the continuity of the mineralized zone and contributed to the expansion of known reserves in the Perau area. Fig. 7a presents the geometry of the mineralized zone and stratigraphic stacking for the Perau Formation based on drill core petrography and electron probe analysis of representative samples.

The drill hole AG-01 has 331.15 m (Fig. 7.b) and intercepts all the lithotypes described by Faleiros *et al*. (2012). The first 235 meters consists of intercalations between (garnet)-(graphite)-quartz-biotite-sericite schist (MP1px) (Fig. 7b - 01) locally with pyrite and disseminated pyrrhotite and metric to decametric levels of metabasic rocks (Fig. 7b – 02) and amphibole schist. Between 235 and 320 meters, the schist unit comprises intercalations of calc-silicate rock (amphibole-carbonate-biotite-schist with and without the mineralized horizon), graphite-sericite schist and centimetric to metric layers of quartzite. From 320 to 331.15 meters, the core is dominated by quartzite.

Magnetite-rich calc-silicate rocks (up to 40%) occur stratigraphically above the mineralized level. This level (Fig. 7b – 03 and 04) is the hanging wall of Pb-Zn-Ag-

(Cu-Ba) mineralizations in the Perau Formation area and is a prospective guide to new occurrences. The mineralized horizon (255.95 - 265.90 m) comprises intense dissemination (locally with massive levels) of galena and sphalerite (Fig. 7b – 05 and 06) in the calc-silicate rocks with minor barite contents. A graphite-sericite-schist occurs along a ductile-brittle shear zone below the mineralized horizon (265.90 - 272.00 m), which was described by Daitx *et al.* (1983) as the footwall of mineralization.

4.3.2 Canoas Mine Area

The mineralized horizon in the Canoas mine area occurs near the contact of the lens of calc-silicate rocks with the basal quartzite. The quartzite range from pure to micaceous, with a marked mineral stretching lineation. There is no evidence of a copper mineralized level above the calc-silicate rocks as it occurs in the Perau mine region.

The stratigraphy of the mineralized horizon observed inside the Canoas 01 mine (Fig. 4) comprises, from the bottom to the top: a level of barite-phlogopite-carbonate schist with disseminated sulfides (Fig. 8a and Fig. 8b), followed by a level rich in oxidized copper and barite associated to the calc-silicate rock (Fig. 8c); disseminations and massive levels with galena, sphalerite and other sulfides associated with calc-silicate rock (Fig 8d and Fig. 8e); and mineralization associated with silica-rich levels (Fig. 8f).

The mineralization associated with calc-silicate rocks is characterized by some centimetric levels of massive sulfide (Fig. 8e) and by galena, sphalerite, chalcopyrite, and pyrite spreads. A silica-rich level presents disseminated sphalerite, galena and pyrite.

In addition to the information obtained in the galleries, other features associated with the mineralized range were found in the vicinity of the mines. Carbonate-amphibole-magnetite schist, locally with garnet, occurs near the mine of Canoas 01. This rock is inferred as a magnetic banded iron formation in the hangingwall of mineralizations associated with the Perau Horizon.

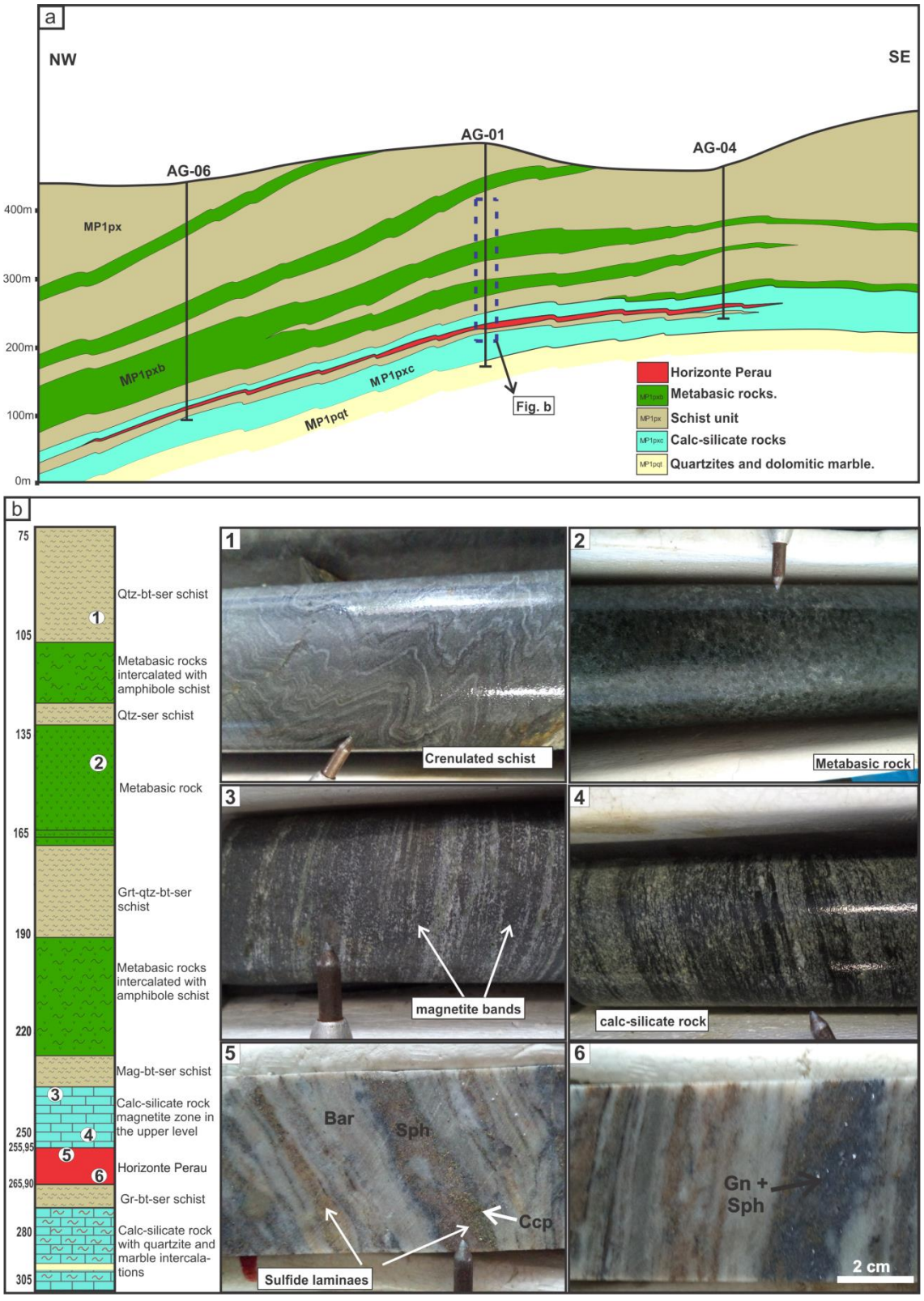

Fig. 7. (a) Geological section showing the correlation between AG-01, AG-04, and AG-06 drill holes that intercepted the mineralized zone (Perau Horizon). Dashed red lines correspond to the drill hole AG-01 described in b; (b) A schematic description of part of drill hole AG-01, along with the mineralized Horizonte Perau; b (1-6) core samples of different stratigraphic levels of Perau Formation, intercepted by drill hole AG-01. Bar: barite; Sph: sphalerite; Ccp: chalcopyrite; Gn: galena.

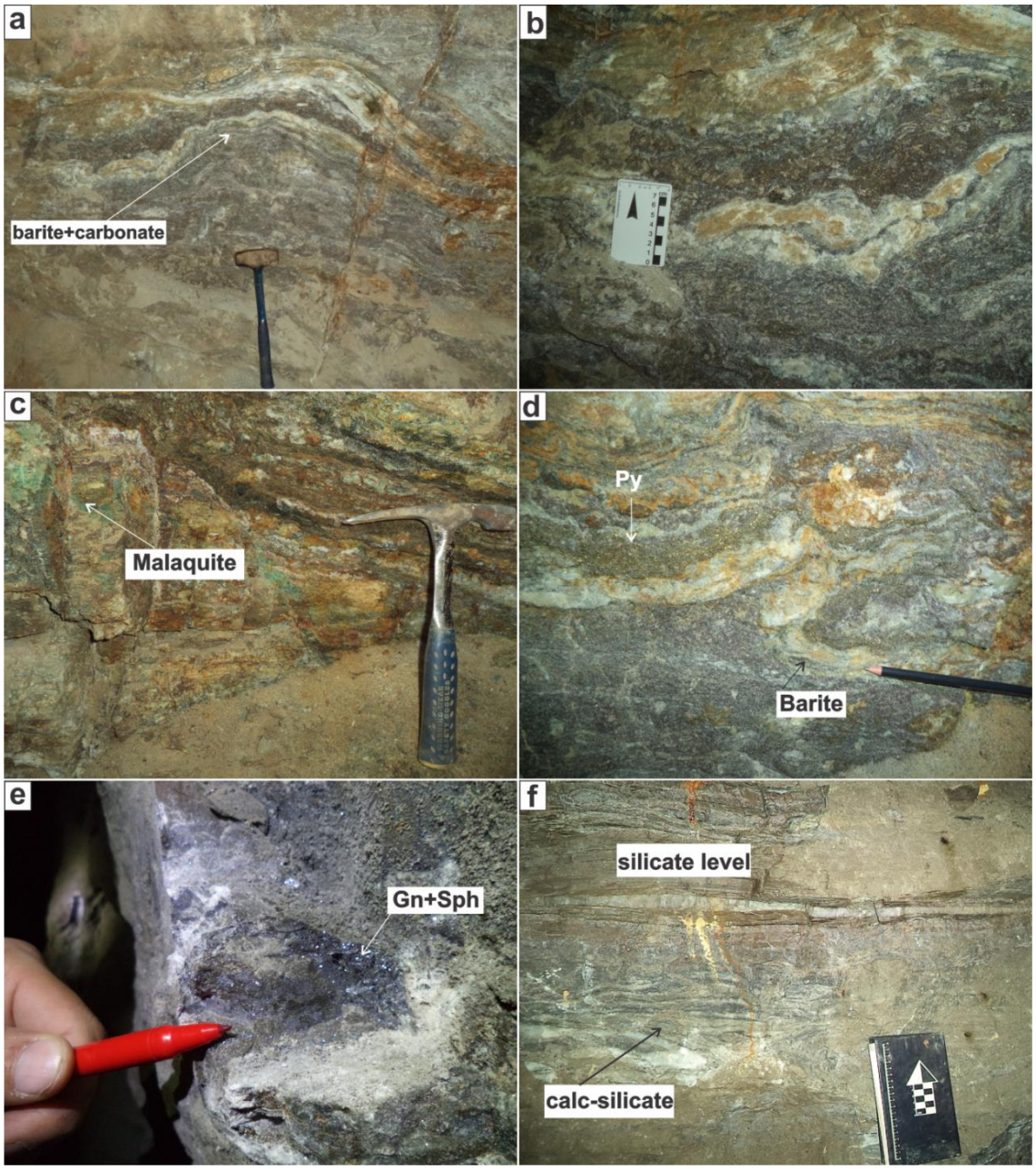

Fig. 8. Features of mineralization in the mine of Canoas 01. (a-b) Levels of barite-phlogopite-carbonate schist with disseminated sulfides; (c) oxidized copper associated to the calc-silicate rock with barite; (d) level of folded massive sulfide (pyrite); (e) detail of massive sulfide with galena and sphalerite; (f) Contact between calc-silicate rich ore and silica-rich ore. Gn: galena; Sph: sphalerite.

Microscopic analysis of different ore levels collected at the Canoas mine shows the mineralization is hosted by calc-silicate rocks primarily composed of tremolite, phlogopite, quartz, barite, and sulfides (Fig. 9a-l). Texturally, the rocks present a range of metamorphic textures, from granoblastic and lepidoblastic textures with associated recrystallization microstructures such as formation of quartz sub grains rotation. Sulfide remobilization textures(e.g. sulfide veilents) are also present and are generally similar to those observed in the Perau Mine area. The ore is primarily characterized by galena and

sphalerite associated with calc-silicate and silicate-rich ore, chalcopyrite associated with the copper-rich level and pyrite on the silica-rich level (Fig. 9c, f, i and j). However, all the sulfides occur at different levels.

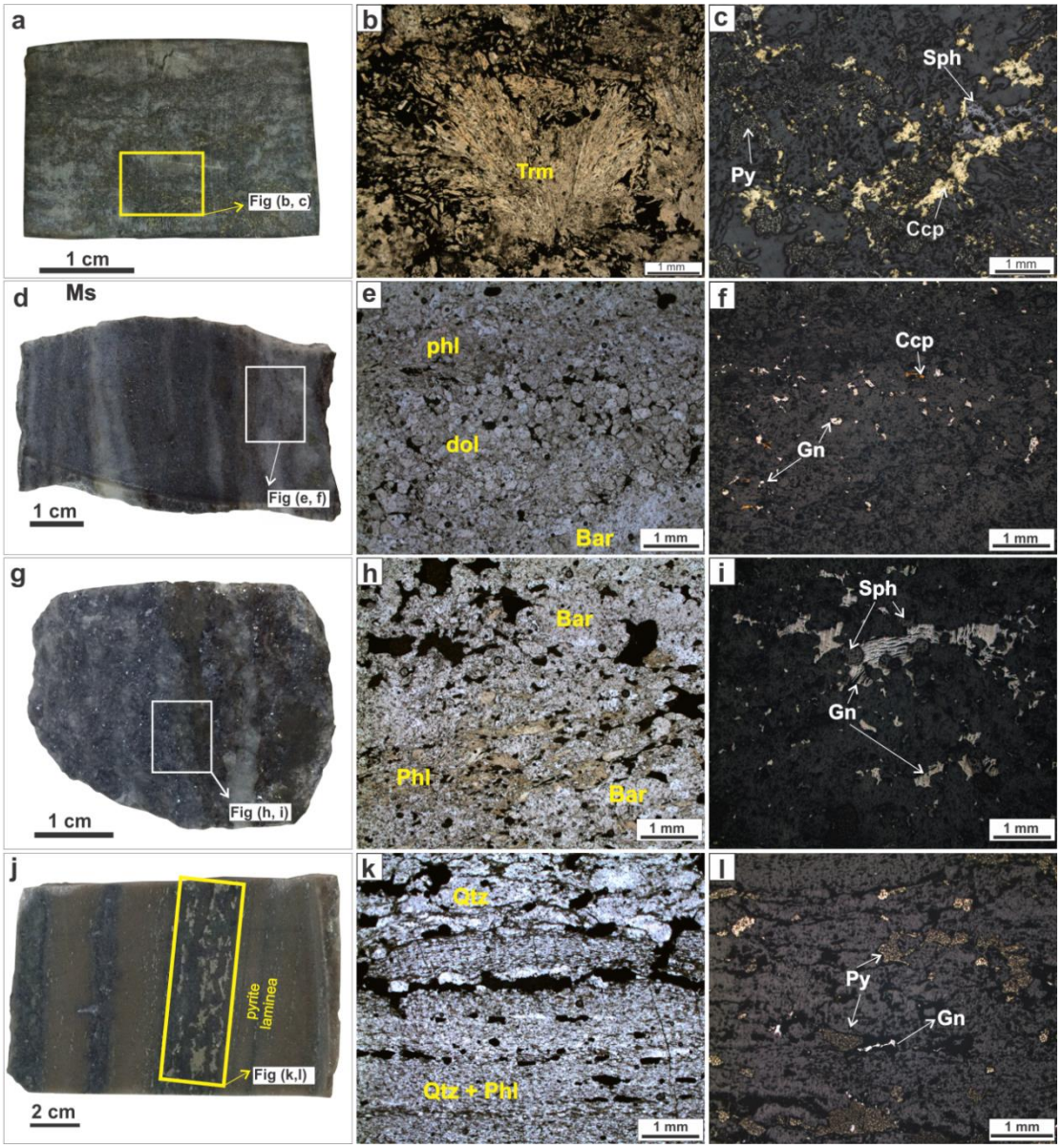

Fig. 9. Hand specimen (a, d, g, and j) photomicrograph of different levels of mineralization in the Canoas mine; transmitted light (b, e, h, and K) showing textural relations between gangue minerals and ore minerals; and reflected light photomicrograph showing the principal features of mineralization in the mine of Canoas. Bar: barite; Ccp: chalcopyrite; dol: dolomite; Gn: galena; Phl: phlogopite; Py: pyrite; Qtz: quartz; Sph: sphalerite.

4.4. Analytical Methods

A total of 10 ore samples of the mineralized zone of the Canoas mine were analyzed at SGS Geosol Laboratórios Ltda, Brazil. Determinations of the concentrations of the major elements (SiO_2, TiO_2, Al_2O_3, Fe_2O_3, MgO, CaO, MnO, Na_2O, K_2O, P_2O_5) were obtained employing X-ray fluorescence (XRF). For the determination of the trace

elements, total digestion of the samples was initially performed by dissolution using HNO_3, HF, $HClO_4$, and HCl or by melting with lithium metaborate. Subsequently, the samples were analyzed by Inductively Coupled Plasma Spectrometry (ICP-MS) and Inductively Coupled Plasma Emission Spectrometry (ICP-OES). The concentrations of Au, Pt, and Pd elements were obtained by the fire assay method with ICP-OES reading and the Ag element by Atomic Absorption Spectrometry (ASA).

Chemical composition of sulfide minerals was determined by Electron Microprobe micro-analyses (EPMA) from 6 thin-polished sections, at the Federal University of Goias (Brazil) using a JEOL model JXA-8230 microprober, operating with an acceleration voltage of 20 kV and 40 nA. The analysis time varied from 10 to 30 seconds, according to the expected abundance of each element in the mineral.

Sulfur isotope data were obtained from galena, sphalerite, chalcopyrite, and pyrite from a total of 13 samples from the polymetallic mineralizations of Canoas Mine and in the samples of the drill holes of Anta Gorda Project. Nearly pure sulfides were obtained after sample crushing with a micro drill, by handpicking using a binocular microscope. The results are presented in per thousand (‰) using the delta (δ) notation and referred V-CDT (Canyon Diablo Troilite) for sulfur, standards

The analyses were carried out at the University of Brasília (Brazil). For sulfur analysis, SO_2 was produced by combustion of about 0.5 mg of sample loaded into tin capsules reacting at 1080 C. The combusted gases were carried in a He stream and reduced by contact with high-purity copper wires and the SO2 was separated by gas chromatography. Analyses were done by the EA-IRMS (Elemental Analysis e Isotope Ratio Mass Spectrometry), using a Flash Elemental Analyzer and ThermoFisher MAT 253 mass spectrometer. Uncertainties are estimated at 0.2‰.

A total of 61 thin-polished sections of the mineralized horizon and their host rocks were studied during the petrographic analyses, and the paragenesis of the gangue and ore minerals are determined based on their textural relationship. From this total of described thin-polished sections, we selected the best representative intervals for fluid inclusions studies.

Fluid Inclusion petrography and microthermometric analyses were accomplished on 8 doubly-polished sections (100 μm thick) of the polymetallic mineralizations of Canoas Mine and in samples of drill holes of Anta Gorda Project (AG-01, AG-02, AG-04 e AG-05) using a Linkan heating-freezing stage THMSG 600, which has been calibrate with CSCO2 standard. The precision estimates were ± 0.1 ºC for temperatures

of CO2 homogenization (ThCO2), and CO2 melting (TmCO2), ± 0.2 ºC for clathrate dissociation (TdCl) and ice melting (TmIce), ± 1 ºC for eutectic melting of aqueous-carbonic and aqueous inclusions (TE) and ± 2 ºC for total homogenization (Th). Physico-chemical properties of trapped fluids and isochores were calculated with the computer software packages FLUIDS and CLATHRATES (Bakker, 1997, 2003), applying state equations for determining the composition and density of CO2-rich inclusions and carbonic phases of H2O-CO2 inclusions (Duschek *et al.*,1990; Span and Wagner, 1996); density and salinity of aqueous phases, as well as bulk properties of H2O-CO2 inclusions (Duan *et al.*, 1992a, b); bulk properties and densities (Zhang and Frantz, 1987) and the volumetric proportions of aqueous fluid inclusions (Archer, 1992).

4.5. Results

4.5.1 Geochemistry of the ore samples

Geochemical analyses of 10 ore samples collected in the gallery of Canoas 01 mine from the massive, silica-rich, and barite-rich ore levels exhibit a composition dominated for Pb-Zn-Ba. The ore presents high Cu content, reaching up to 0.478 wt.%. Silver is another economic feature of this deposit with samples presenting grades in the order of 159 ppm. No ore geochemistry studies were conducted in the galleries of the Perau mine areas due to the impossibility of access. However, previous studies have attested to the polymetallic aspect of this deposit (Daitx, 1996). Mineralogical observations and electron probe micro-analysis (EPMA) were performed in the order of determining mineral composition and distribution of Ag, Co, Ni, Cu, and Au in the sulfides of ore samples.

Table 1: Concentrations of the major (wt.%) and minor elements (ppm) of Canoas 01 ore samples.

Canoas											
		Barite-rich ore				Massive ore				Silica-rich ore	
		1	2	3	4	1	2	3	4	1	2
Pb	wt.%	3.88	1.82	2.68	2.17	6.93	5.47	8.11	4.25	0.95	1.00
Zn	wt.%	5.35	3.05	1.75	4.27	2.8	5.99	18.66	10.63	0.34	0.96
Ba	wt.%	1.19	2.32	2.9	2.58	1.81	1.74	0.78	0.64	0.73	2.46
Fe	wt.%	3.05	2.13	1.12	3.36	1.48	2.68	4.00	4.68	6.49	9.02
Ca	wt.%	3.05	4.44	2.36	8.11	0.79	1.3	2.54	0.65	3.49	3.25
Mg	wt.%	1.62	2.41	1.11	4.06	0.83	2.36	1.53	0.6	1.81	2.18
Cu	ppm	168.1	186.1	399.1	448.8	35.8	322.6	181.5	196.4	4786	708.3
Ag	ppm	126	149	88	38	159	116	108	77	143	27
As	ppm	<1	<1	<1	<1	3.00	22	<1	3.00	<1	<1
Ni	ppm	32	88.2	44.3	19.8	60	44.1	68.4	108.8	14.2	49.1
Mo	ppm	1.47	0.82	<0.05	0.93	1.08	0.37	2.3	3.06	1.95	6.23
Bi	ppm	2.82	1.95	2.11	2.41	2.41	2.21	2.41	2.13	15.24	2.39
Au	ppb	15	228	<5	14	36	20	6	<5	<5	<5

4.5.2 Sulfide mineral chemistry

The compositions of sulfide minerals (e.g., galena, sphalerite, chalcopyrite, and pyrite) were determined by the analyses of 6 samples from the mineralized calc-silicate (barite-rich and silica-rich ores) and massive levels in the Canoas and Perau deposits. The results of the representative electron microprobe micro-analyses (EPMA) are shown in Tables 2 and 3.

4.5.2.1 Galena

Galena is the most abundant ore mineral occurring in the deposits of Perau and Canoas closely associated with sphalerite. It is characterized by domains formed by irregular masses partially encompassing other sulfides (Fig. 10a and Fig. 10b). Microprobe analysis shows the Ag contents are usually below the detection limit. However, in a few grains contents up to 13.22 wt.% Ag was detected (Fig. 10c).

4.5.2.2 Sphalerite

Sphalerite is closely associated with galena, and appears in all levels of the mineralization, occurring as polygranular irregular masses with subhedral grains (Fig. 10d). Replacement of pyrite and chalcopyrite by sphalerite is a common feature in these deposits, being an indicator of sulfides precipitation timing. Different colors of intern reflections between ore rich in barite (yellowish) and ore rich in silica (reddish) reflect

the iron content in these different levels (Table 4). The EPMA results show the sphalerite from barite-rich ore has a low content of Fe (avg. 1.22 wt.%), while the sphalerite from silica-rich ore show enrichment in Fe with an average of 7.24 wt.%. Co values are higher in the barite-rich ore (avg. 0.47 wt.%) than in silica-rich ore (avg. 0.01 wt.%). The Ag, Sb, and Ni contents are low for the two ores (Table 2). Data obtained by Daitx (1996) show averages Zn/Cd ratio of 259.3 wt.% and 410.5 wt.% for barite-rich ore and silica-rich ore, respectively.

4.5.2.3 Chalcopyrite

Chalcopyrite is a common ore mineral in the Pb-Zn deposits of the Perau Formation and has been described in all stratigraphic levels of the mineralization, highlighting the copper level above the Perau Horizon. Textural relationships indicate chalcopyrite generally replaces pyrite and was replaced by sphalerite and galena, as suggested by chalcopyrite disease textures in sphalerite grains (Fig. 10e and Fig. 10f). The EPMA results (Table 3) show the chalcopyrite composition is nearly pure, with Pb and Ag being detected in small quantities, an average of 0.10 and 0.03 wt. %, respectively.

4.5.2.4 Pyrite

Pyrite is the less abundant sulfide in the Perau and Canoas deposits. This mineral occurs as euhedral to anhedral coarse-grained crystals in the host rocks and as medium- to fine-grained euhedral and anhedral grains coexisting with the other sulfides in the massive and disseminated ore levels. Inclusions in chalcopyrite and galena represent relics of replacement (Fig. 10e). EPMA analyses (Table 3) shows nearly constants Pb (avg. 0.14 wt.%), Zn (0.01 wt.%) and Cu (0.01 wt.%) contents. However, Ni (avg. 0.01 against 0.18 wt.%) and As (avg. 0.06 against 0.73 wt.%) show variations between samples from the Canoas and Perau deposits, respectively.

Table 2: EPMA element concentrations (wt%) for sphalerite (Sph) and galena (Gn) of Perau and Canoas deposits.

Deposit	Min.	S	Fe	Pb	Zn	Cu	Ag	As	Co	Ni	Mn	Au	Sb	Total
Perau	Sph	32.98	7.05	0.02	57.48	0.24	bdl	0.02	0.43	0.00	0.03	bdl	bdl	98.26
Perau	Sph	33.53	7.25	0.04	57.21	0.07	bdl	bdl	0.46	bdl	0.03	bdl	0.01	98.59
Perau	Sph	33.31	7.66	0.05	57.05	0.01	bdl	bdl	0.54	0.00	0.04	bdl	0.01	98.68
Perau	Sph	33.02	6.69	0.04	57.60	0.11	bdl	bdl	0.42	bdl	0.03	bdl	0.00	97.89
Perau	Sph	32.94	7.56	0.04	56.75	0.17	bdl	bdl	0.48	0.01	0.04	bdl	bdl	98.00
Perau	Sph	32.58	1.23	0.00	64.47	0.06	bdl	0.01	0.01	bdl	bdl	bdl	bdl	98.35
Perau	Sph	32.79	1.26	0.04	64.65	bdl	bdl	bdl	0.00	0.00	0.01	bdl	0.00	98.75
Perau	Sph	32.76	1.26	0.06	64.25	bdl	0.00	bdl	0.01	0.001	bdl	bdl	bdl	98.33
Perau	Sph	32.82	1.19	0.04	64.68	0.00	bdl	bdl	bdl	0.001	0.007	bdl	0.02	98.76
Perau	Sph	32.24	1.19	0.09	63.96	0.00	0.00	bdl	bdl	0.011	0.005	bdl	bdl	97.50
	Avg.	**32.90**	**4.23**	**0.04**	**60.81**	**0.08**	**0.00**	**0.01**	**0.29**	**0.00**	**0.02**	**-**	**0.00**	**98.31**
Canoas	Gn	13.35	bdl	85.87	0.01	0.00	bdl	bdl	0.01	bdl	0.00	bdl	0.03	**99.27**
Canoas	Gn	13.21	0.00	83.99	bdl	bdl	bdl	bdl	0.00	bdl	0.01	bdl	bdl	**97.21**
Canoas	Gn	13.16	0.00	84.28	0.02	0.01	bdl	bdl	bdl	bdl	bdl	bdl	0.04	**97.51**
Canoas	Gn	13.31	0.00	84.36	bdl	bdl	bdl	bdl	bdl	0.00	bdl	bdl	bdl	**97.68**
Canoas	Gn	13.30	0.01	85.11	0.01	bdl	bdl	bdl	bdl	0.01	bdl	bdl	0.02	**98.46**
Canoas	Gn	13.22	bdl	84.76	0.01	bdl	bdl	bdl	bdl	0.00	0.00	bdl	0.00	**97.99**
Canoas	Gn	13.10	bdl	84.09	bdl	bdl	bdl	bdl	0.00	0.01	bdl	bdl	0.02	**97.22**
Canoas	Gn	13.25	0.00	83.99	0.01	bdl	bdl	bdl	0.00	bdl	0.00	bdl	0.01	**97.26**
Canoas	Gn	13.23	bdl	85.31	bdl	0.02	bdl	bdl	0.01	0.00	bdl	bdl	bdl	**98.56**
Canoas	Gn	13.11	bdl	84.27	0.02	0.00	bdl	bdl	bdl	0.01	bdl	bdl	0.02	97.43
Canoas	Gn	13.13	bdl	84.24	bdl	0.00	bdl	bdl	bdl	bdl	bdl	0.012	0.02	97.41
Canoas	Gn	14.11	bdl	73.74	0.02	0.00	13.22	bdl	bdl	bdl	0.00	bdl	bdl	101.09
Canoas	Gn	13.50	0.01	78.62	0.02	bdl	8.65	bdl	bdl	bdl	0.00	bdl	bdl	100.80
Canoas	Gn	13.23	bdl	83.59	0.01	bdl	bdl	bdl	bdl	bdl	bdl	bdl	0.02	96.85
Canoas	Gn	13.30	bdl	84.70	0.02	bdl	0.54	bdl	bdl	bdl	bdl	bdl	0.01	98.57
Canoas	Gn	13.24	bdl	84.26	0.02	bdl	bdl	bdl	0.01	bdl	0.01	bdl	0.02	97.55
	Avg.	**13.30**	**0.00**	**83.45**	**0.01**	**0.01**	**1.40**	**-**	**0.00**	**0.01**	**0.00**	**0.01**	**0.02**	**98.18**
Perau	Gn	13.18	bdl	84.33	bdl	0.01	bdl	bdl	bdl	0.01	bdl	bdl	0.00	97.53
Perau	Gn	13.33	bdl	84.84	bdl	0.00	bdl	bdl	0.00	bdl	0.00	bdl	0.00	98.18
Perau	Gn	13.12	0.00	84.82	0.00	0.00	bdl	bdl	bdl	bdl	0.01	bdl	0.01	97.96
Perau	Gn	13.15	bdl	84.58	0.02	0.03	bdl	bdl	bdl	0.00	0.01	bdl	0.00	97.79
Perau	Gn	13.18	bdl	84.80	0.02	0.00	bdl	bdl	0.01	bdl	bdl	bdl	0.04	98.04
Perau	Gn	13.23	bdl	84.89	bdl	0.00	bdl	bdl	bdl	0.01	0.00	bdl	0.04	98.17
Perau	Gn	13.34	bdl	85.74	bdl	0.00	bdl	bdl	bdl	0.01	bdl	0.01	0.01	99.10
Perau	Gn	13.29	0.01	85.46	0.00	0.00	bdl	bdl	bdl	0.00	bdl	bdl	0.01	98.78
Perau	Gn	13.26	bdl	85.10	bdl	0.00	bdl	bdl	bdl	bdl	0.01	bdl	0.00	98.36
Perau	Gn	13.24	0.00	84.89	bdl	0.01	bdl	bdl	bdl	0.00	bdl	bdl	0.02	98.16
Perau	Gn	13.16	bdl	84.94	0.02	0.01	bdl	bdl	0.01	bdl	0.00	bdl	0.02	98.17
Perau	Gn	12.96	bdl	85.17	0.00	0.00	bdl	bdl	0.01	bdl	0.00	bdl	0.00	98.14
Perau	Gn	13.17	bdl	84.91	bdl	0.00	bdl	bdl	bdl	0.01	bdl	bdl	0.00	98.09
Perau	Gn	13.09	bdl	85.35	0.02	0.01	bdl	bdl	0.00	0.00	bdl	bdl	0.01	98.48
Perau	Gn	13.17	0.01	85.21	0.00	0.00	bdl	bdl	0.00	0.02	bdl	bdl	0.02	98.43
Perau	Gn	13.30	0.01	85.25	0.01	0.00	bdl	bdl	bdl	bdl	bdl	bdl	0.04	98.60
Perau	Gn	13.34	0.03	85.26	bdl	0.01	bdl	bdl	bdl	bdl	bdl	bdl	0.02	98.66
Perau	Gn	13.58	0.00	84.19	0.01	0.02	bdl	bdl	bdl	bdl	bdl	bdl	0.04	97.84
Perau	Gn	13.17	0.01	85.43	bdl	0.01	bdl	bdl	0.01	bdl	0.00	bdl	0.00	98.64
Perau	Gn	13.22	bdl	85.18	bdl	0.03	bdl	bdl	bdl	0.00	bdl	bdl	0.02	98.45
	Avg.	**13.22**	**0.01**	**85.02**	**0.01**	**0.01**	**-**	**-**	**0.01**	**0.01**	**0.00**	**0.01**	**0.01**	**98.28**

bdl= below detection limit

Table 3. EPMA element concentrations (wt%) for chalcopyrite (ccp) and pyrite (py) of Perau and Canoas deposits.

Deposit	Min.	S	Fe	Pb	Zn	Cu	Ag	As	Co	Ni	Mn	Au	Sb	Total
Perau	Cpy	34.49	30.04	0.11	bdl	33.86	0.042	0.02	0.02	bdl	0.00	0.01	bdl	98.59
Perau	Cpy	34.99	30.04	0.12	bdl	33.50	0.034	bdl	0.04	bdl	0.00	0.00	bdl	98.72
Perau	Cpy	34.85	29.94	0.11	bdl	34.03	0.038	bdl	0.04	bdl	0.00	0.01	bdl	99.02
Perau	Cpy	34.44	29.41	0.14	bdl	33.31	0.039	bdl	0.03	bdl	0.00	0.02	bdl	97.39
Perau	Cpy	34.81	29.97	0.10	bdl	33.76	0.035	bdl	0.04	0.0	bdl	bdl	bdl	98.71
Perau	Cpy	34.46	29.75	0.09	bdl	33.75	0.037	bdl	0.07	bdl	bdl	0.01	bdl	98.17
Perau	Cpy	33.95	29.97	0.06	bdl	33.36	0.025	bdl	0.07	0.0	bdl	bdl	bdl	97.44
Perau	Cpy	34.53	29.95	0.08	bdl	33.55	0.025	bdl	0.04	bdl	bdl	0.01	bdl	98.19
Perau	Cpy	34.24	29.17	0.06	bdl	32.85	0.026	bdl	0.09	0.1	bdl	0.01	bdl	96.56
Perau	Cpy	34.44	28.87	0.11	bdl	33.01	0.017	bdl	0.03	bdl	0.00	bdl	bdl	96.48
Perau	Cpy	34.51	28.99	0.09	bdl	33.07	0.034	bdl	0.03	bdl	0.00	bdl	bdl	96.72
Perau	Cpy	34.65	29.71	0.18	bdl	33.40	0.018	bdl	0.03	bdl	bdl	0.01	bdl	98.01
	Avg.	**34.53**	**29.65**	**0.10**	**-**	**33.45**	**0.03**	**0.00**	**0.04**	**0.01**	**0.00**	**0.01**	**-**	**97.83**
Canoas	Py	52.84	45.26	0.16	0.01	bdl	bdl	bdl	0.40	0.01	bdl	0.00	bdl	98.69
Canoas	Py	53.32	45.30	0.17	0.02	bdl	0.00	0.10	0.96	0.01	bdl	0.01	bdl	99.88
Canoas	Py	54.13	45.89	0.09	bdl	0.01	0.01	0.11	0.52	0.01	bdl	0.02	bdl	100.78
Canoas	Py	53.92	45.61	0.13	bdl	0.02	0.01	0.04	0.34	bdl	bdl	0.01	0.01	100.07
	Avg.	**53.55**	**45.52**	**0.14**	**0.01**	**0.01**	**0.00**	**0.06**	**0.55**	**0.01**	**-**	**0.01**	**0.00**	**99.85**
Perau	Py	52.99	40.68	0.14	0.00	0.02	bdl	3.00	4.96	0.16	0.00	bdl	bdl	101.96
Perau	Py	53.22	45.21	0.12	bdl	0.03	bdl	0.00	0.08	0.44	bdl	0.01	bdl	99.12
Perau	Py	53.30	45.37	0.12	bdl	0.03	bdl	bdl	0.09	0.19	bdl	bdl	bdl	99.10
Perau	Py	52.99	42.35	0.12	0.00	0.01	bdl	2.69	3.18	0.39	bdl	bdl	bdl	101.73
Perau	Py	52.32	42.17	0.14	bdl	bdl	bdl	2.66	3.21	0.39	bdl	0.03	bdl	100.91
Perau	Py	52.48	42.56	0.12	0.01	0.00	bdl	2.69	2.84	0.35	bdl	0.01	bdl	101.07
Perau	Py	54.34	45.44	0.20	bdl	0.00	bdl	bdl	0.05	bdl	bdl	bdl	bdl	100.05
Perau	Py	54.30	45.66	0.13	bdl	bdl	bdl	bdl	0.04	bdl	bdl	0.00	bdl	100.14
Perau	Py	54.12	45.71	0.17	bdl	0.01	bdl	bdl	0.04	0.02	0.00	0.02	bdl	100.09
Perau	Py	53.95	45.72	0.14	0.02	bdl	bdl	0.06	0.34	0.09	bdl	bdl	0.01	100.31
Perau	Py	54.14	45.62	0.17	bdl	bdl	0.00	0.09	0.36	0.11	0.00	0.04	bdl	100.54
Perau	Py	54.74	45.54	0.11	0.01	0.02	bdl	0.10	0.38	0.08	bdl	bdl	bdl	100.99
Perau	Py	54.92	45.26	0.18	bdl	0.01	0.00	0.11	0.52	0.10	0.00	0.01	bdl	101.12
Perau	Py	54.01	45.49	0.15	bdl	0.01	bdl	0.12	0.45	0.18	bdl	0.00	bdl	100.40
Perau	Py	54.17	45.52	0.12	0.00	bdl	0.00	0.15	0.41	0.24	bdl	0.03	bdl	100.64
Perau	Py	54.63	45.65	0.12	bdl	0.01	bdl	0.07	0.42	0.12	bdl	0.03	bdl	101.06
	Avg.	**53.79**	**44.62**	**0.14**	**0.00**	**0.01**	**0.00**	**0.73**	**1.09**	**0.18**	**0.00**	**0.01**	**0.00**	**100.58**

bdl= below detection limit

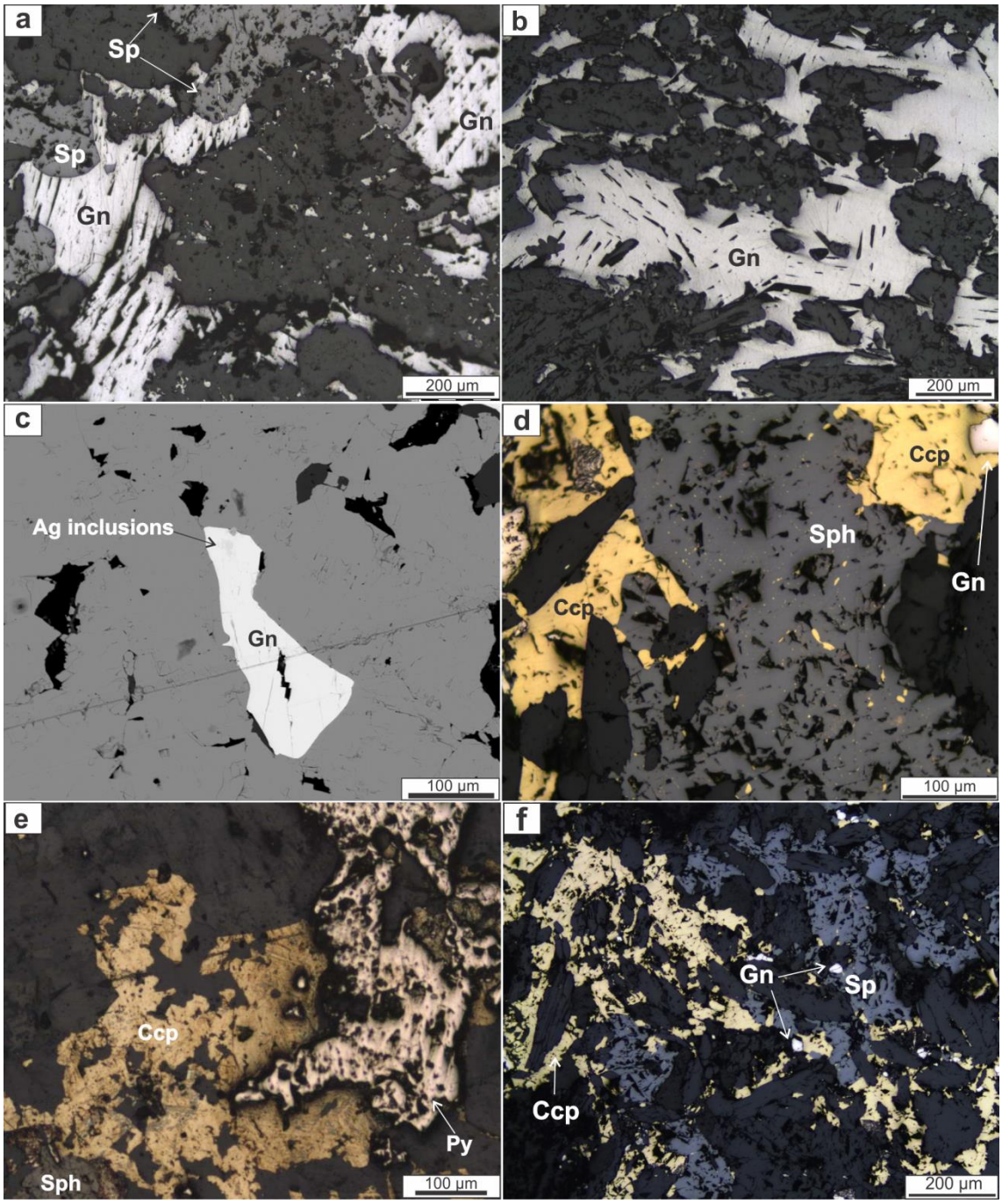

Fig. 10. Reflected light (a, b, d, e, and f) and BSE images (c) showing the textural relationships between the ore-forming minerals. (a) Galena in contact with sphalerite; (b) Mass of interconnected galena aggregate in a brecciated ore; (c) BSE image showing a galena grain with Ag inclusions. (d) Sphalerite grains replacing chalcopyrite; (e, f) Grains of chalcopyrite with pyrite inclusions in contact with a sphalerite grain. Note chalcopyrite inclusions in sphalerite; Sph: sphalerite; Gn: galena; Py: pyrite; Ccp: chalcopyrite.

4.5.3 Sulfur isotopes

We have determined the sulfur isotope composition of 13 samples of ore minerals (pyrite, sphalerite, galena, and chalcopyrite) in the deposits of Canoas and Perau and drill holes of SW-Perau. We also compiled data from previous works (Daitx,

1996; Bettencourt *et al.*, 1992) for sulfides (pyrite, sphalerite, and galena) and sulfate (barite) from the Canoas deposit. The isotopic results are summarized in Table 4 below.

Table 4: The δ34S values of sulfide minerals from Canoas and Perau deposits.

Sample	Mineral	Deposit	$\delta^{34}S$‰	Source
GC-10	Pirite	Canoas	3.9	
GC-31	Pirite	Canoas	3.4	
GC-10	Sphalerite	Canoas	3.3	
GC-30	Sphalerite	Canoas	3.4	Daitx, 1996
GC-27	Galena	Canoas	1.2	
GC-42	Barite	Canoas	20.6	
81/18A	Barite	Canoas	21.5	
GC-10	Barite	Canoas	22.2	
MB-15E	Pirite	Canoas	6.75	
MB-15L	Pirite	Canoas	4.61	
MB-15U	Pirite	Canoas	5.74	
MB-15J	Galena	Canoas	13.16	
MB-15H	Galena	Canoas	16.87	
MB-15H	Sphalerite	Canoas	10.49	
AG-02B	Pirite	Perau	-1.88	
AG-04SD	Pirite	Perau	2.99	
MB-12A	Pirite	Perau	3.25	
AG-01C	Sphalerite	Perau	2.04	
AD-01D	Galena	Perau	1.08	
AG-01C	Galena	Perau	-0.91	
AG-03D	Galena	Perau	2.21	
AD-08B	Chalcopyrite	Perau	0.34	

4.5.3.1 Perau deposit

All sulfides from the Perau deposit, including chalcopyrite from the brecciated copper level, display a limited range of $\delta^{34}S$ from -1.88 to +3.25‰ (Table 4), despite having been collected from different areas and ore types. The main ore minerals, galena and sphalerite have a smaller variation showing $\delta^{34}S$ values from -0.91 to +2.21‰ (Fig. 11).

4.5.3.2 Canoas deposit

The data obtained in the Canoas deposit by Daitx (1996) have a range of S-isotope compositions between 1.2 to +3.9‰ (n=5) (Table 4). These data are in contrast with the data that we obtained, which presents relative enrichment in ^{34}S with values obtained in pyrite ranging from +4.6 to +6.75 ‰, which is similar to the data obtained by Bettencourt *et al.* (1992) with a range of $\delta^{34}S$ clustered among 2.8 to +8.2‰. However, the values of $\delta^{34}S$ in galena and sphalerite show an enrichment with values ranging from +10.49 to +13.16 ‰ (Fig. 11). The determinations from sulfates in barite

of the mineralized zone showed $\delta^{34}S$ values from + 20.6 to 22.2‰ (Fig. 11; Daitx, 1996).

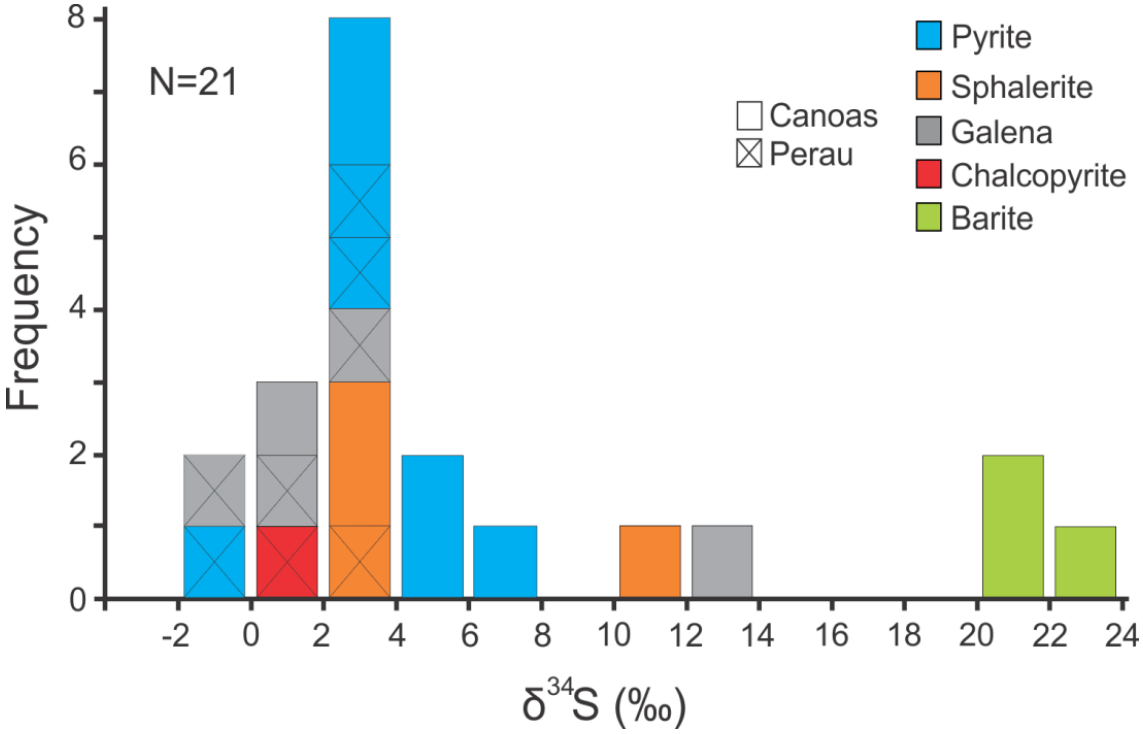

Fig. 11. Frequency distribution of sulfur isotope values for sulfides (pyrite, sphalerite, galena, and chalcopyrite) and ore-associated barite from the deposits of Canoas and Perau. Data from Bettencourt et al. (1992) and Daitx (1996).

4.5.3.3 Isotope thermometry

Using the sulfur isotope compositions of the hydrothermal minerals and the fractionation equations of Ohmoto and Rye (1979) for the sphalerite-galena pair, the temperature has been calculated. The sphalerite-galena pair yielded a temperature value of 227°C in a sample of barite level ore with galena and sphalerite beds.

4.5.4 Fluid Inclusions

Detailed fluid inclusion petrographic has been performed in quartz crystals of 8 double-polished thin sections (100-200 μm-thick) of calc-silicate rocks (barite-rich and silica-rich ore) mineralized with Pb-Zn-Ag(Cu-Ba) of the deposits of Perau and Canoas. From these, 5 samples were selected for microthermometric analyses, including samples with in situ mineralization and with weak deformation. The presence of well-preserved primary and secondary fluid inclusions in quartz grains related to the mineralization and with weak evidence of strain were the criteria adopted for sample selection, once stratigraphic and structural relationships suggest the mineralization precipitations occur before the deformation events. This study has been performed in the more limpid

portions of the host quartz crystals, which present inclusions with sizes bigger than 5 μm, suitable for microthermometric analysis.

4.5.4.1 Fluid inclusion types and assemblages

Three different types of fluid inclusions are recognized based on the number of phases at room temperature and phase changes during freezing-heating runs. The three types of fluid inclusions occur as clusters and trails (Fig. 12a and Fig. 12b). Necking down features are present in all three types (Fig. 12c). In this study, inclusions necked have been avoided.

Type 1 is the most abundant type and consists of primary and secondary fluid inclusions with one (CO_{2vapor}) and two-phase (CO_{2liq} -CO_{2vapor}) carbonic inclusions, which has various shapes (regular, irregular, rounded). These inclusions occur in all samples and are dark, varying from 5 to 20 μm in size. Type 2 consists of primary two-phase (H_2O_{liq}+CO_{2vapor}) and three-phase (H_2O_{liq}+ CO_{2liq}+ CO_{2vapor}) aqueous-carbonic inclusions. The inclusions have sizes from 4 to 30 μm with irregular, and negative crystals shapes. The aqueous phase is generally clear, and the carbonic phase is dark, with CO_2 phase occupying 5 to 80% of the cavities. Type 3 is the least abundant fluid inclusion type occurring along secondary trails and consisting of one (H_2O_{liq}) and two-phase (H_2O_{liq}- H_2O_{vapor}) aqueous inclusions, with sizes between 5 to 20 μm, a clear visual aspect and regular and irregular (rounded to elongated) shapes (Fig. 12f).

Fluid inclusion assemblages (FIAs) are defined as associations of coeval fluid inclusions trapped at about the same time and petrographically associated (Goldstein and Reynolds, 1994). Applying the definition of FIA, three assemblages have been recognized in the mineralized calc-silicate rocks of Perau Formation: FIA-1 (primary carbonic, aqueous-carbonic, and rare aqueous inclusions; Fig 12a-c), FIA-2 (secondary carbonic inclusions; Fig. 12d-e), and FIA-03 (secondary aqueous inclusions). The plot of Th (temperature of homogenization) versus salinity (wt.% NaCl) is used two show the distinctive characteristics of FIA-01 and FIA-03 (Fig. 13i).

4.5.4.2 Microthermometric results

The CO_2-bearing fluid inclusions (type 1 – FIA-01 and FIA 02) show melting of solid CO_2 ($TmCO_2$) between –57.8° and –56.6°C (Fig. 13a), indicating CO_2 is the dominant volatile in the carbonic phase and only minor amounts of other volatiles like CH_4 and N_2. The CO_2 homogenization ($ThCO_2$) occurred into the liquid state in the

ranges of 4.4-27.4 ºC (FIA-1) and 3.4-28.9 ºC (FIA-2) (Fig 13.b). The calculated densities using the equations of Brown and Hagemann (1994) vary from 0.66 to 0.89 g/cm3 for primary fluid inclusions and from 0.63 to 0.90 g/cm^3 for secondary fluid inclusions, with average at 0.79 and 0.73 g/cm3, respectively.

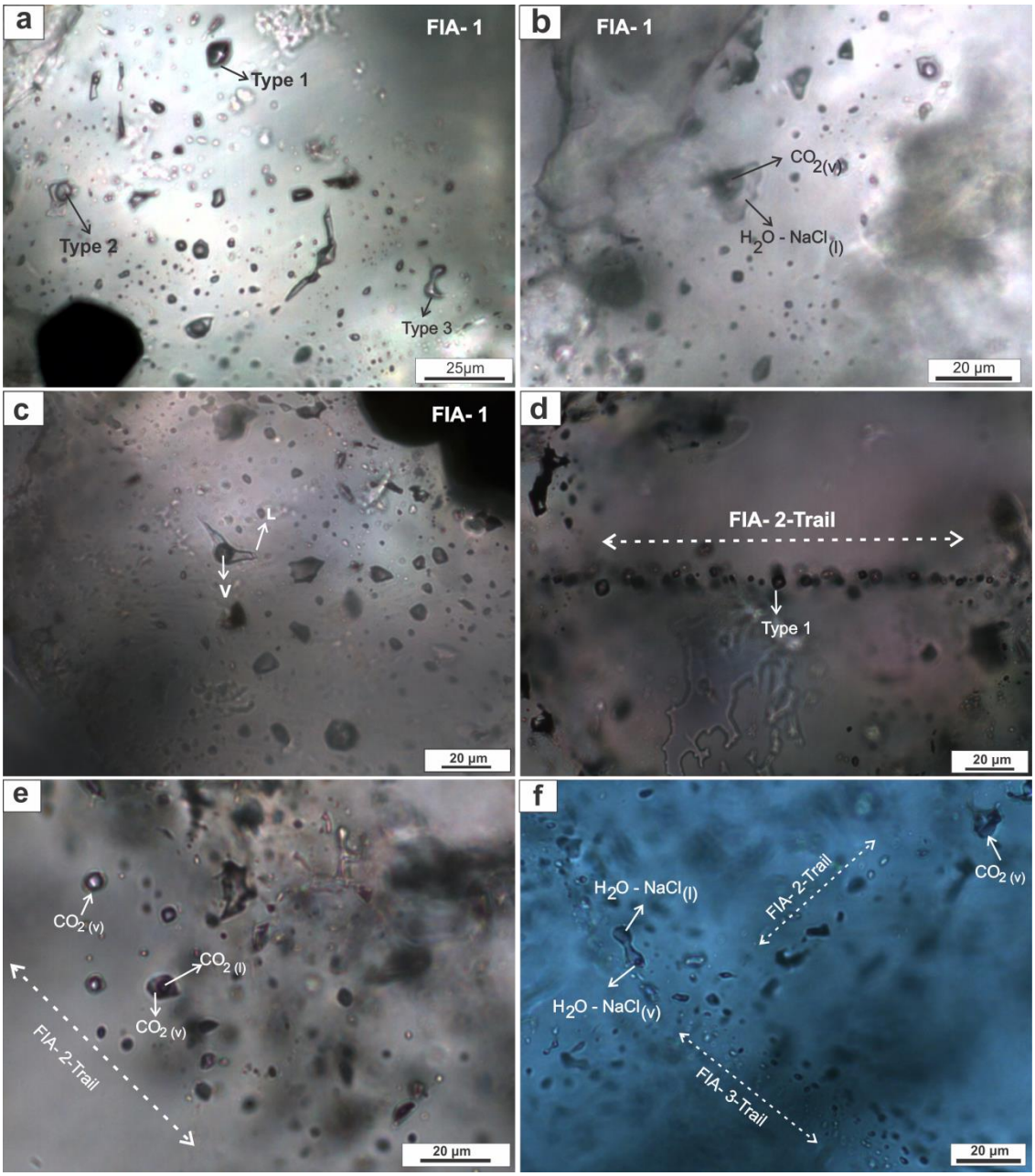

Fig. 12. Aspects of the fluid inclusions. (a and b) Mode of occurrence of FIA-01 fluid inclusions in a single microscopic domain; (c) necking down features in type 2 fluid inclusions; (d-f) Mode of occurrence of secondary FIA-02 and FIA-03 fluid inclusions.

Aqueous-carbonic inclusions (FIA-01; type 2) show T_mCO_2 values between –59.8 to -57.1 °C (Fig 13a), which suggests that CO_2 is the major constituent of carbonic phase with minor amounts of other volatile species (such as CH_4 and N_2). The clathrate dissociation occurs in a range of 4.0 to 12°C (Fig. 13g), corresponding to salinities

between 0.24 to 10.62 wt. % NaCl eq (Fig. 13h). Most of the values are clustered between 8.7-10.9°C, with salinities in a range of 0.45 to 2.35 wt. % NaCl equiv. Homogenization of CO_2 (T_hCO_2), into a liquid state, varies within 7.3 to 21.2°C (Fig. 13b), yielding densities of 0.78 to 0.95 g/cm^3. Eutectic initial melting temperature occurs from -27.7 to -37.2 °C (Fig. 13c), which suggests a system composed of H_2O-NaCl-$MgCl_2$-CO_2. The final homogenization temperatures (T_h) varies from 255 to 401°C (Fig. 13f), into the liquid and vapor state, with a peak between 325-350°C.

The aqueous inclusions (type 3; FIA-03 and rare inclusions in FIA-01), show eutectic temperatures between -59.2 to -67.5°C. The ice melting temperatures (Tm_{ice}) range from -24.6 to -4 ºC (Fig. 13d), indicating salinities between 6.44 and 25.33 wt.% NaCl equiv. (Fig. 13e). The frequency distribution of salinity is bimodal, with peaks at about 10-13 and 20-22 wt.% NaCl equivalent. The total homogenization occurs between 108 and 203°C, with data concentration at 150-175°C (Fig. 13f). Primary aqueous fluid inclusions of FIA-01 show homogenization temperatures between 355 to 391 °C, similar to the data obtained for primary aqueous-carbonic fluid inclusion (FIA-01). The physicochemical data of each assemblage is summarized in Table 5.

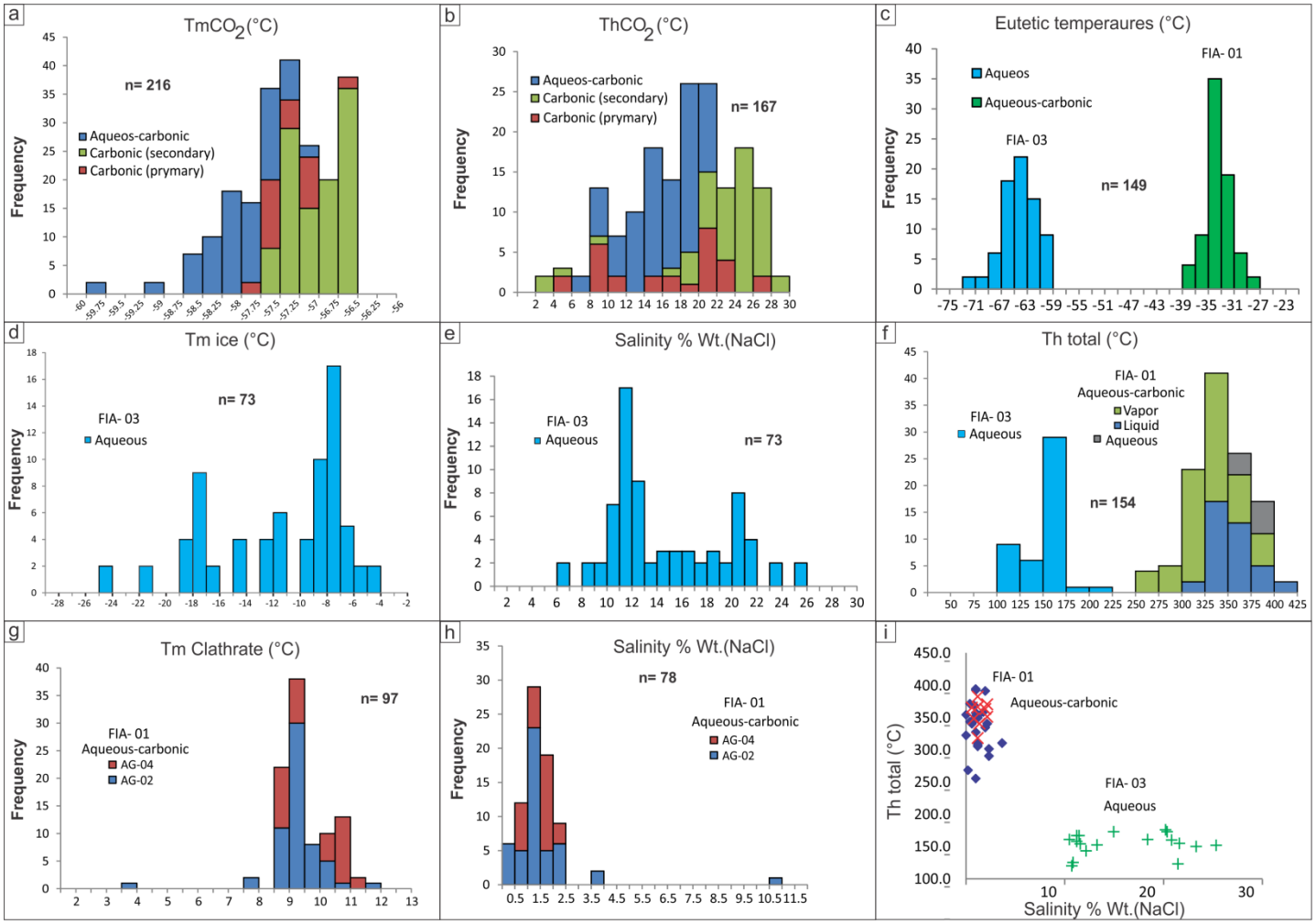

Fig. 13. (a-h) Histograms showing microthermometric data obtained on FIA-01, FIA 02, and FIA-03 of the mineralized calc-silicate rocks of Perau Formation; (i) The plot of salinity %wt. (NaCl) versus homogenization temperature for FIA-01 and FIA 03 inclusions.

Table 5. Summary of microthermometric fluid inclusion data from Canoas and Perau deposits.

FIA	Fluid System	Mode of Ocurrence	$TmCO_2$ (°C)	$ThCO_2$ (°C)	TmCL (°C)	TE (°C)	Tm ice (°C)	Th (°C)	Salinity (wt.% equivalent)	Sample
1	H_2O-NaCl-$MgCl_2$-CO_2	Cluster	-59.8 to -57.2	7.3 to 21.2	4.0 to 12.0	-27.7 to -37.2	-	255 to 394 V 322 to 401 L	0.24 to 10.62 0.45 to 2.35 (most of values range)	AG-04H; AG-05E; AG-02D.
	CO_2-N_2-CH_4		-57.8 to -56.6	4.4 to 27.4						AG-04H; AG-05E; AG-02D.
	H2O-NaCl*							355 to 391L		AG-04H; AG-02D.
2	CO_2-N_2-CH_4	Trail	-57.7 to -56.6	3.4 to 28.9						MB-015L; AG-05E
3	H2O-NaCl-CaCl2	Trail				-59.2 to -70.7	-24.6 to -4.0	108 to 203L	6.44 to 25.33	MB-015L

*Only a few inclusions have been described.

5. DISCUSSION

The integration of the data obtained in this work and available from the literature (Silva et al., 1981; MMAJ-JICA, 1981, 1982, 1983, 1984; Daitx et al., 1983; Daitx, 1984, 1996) helped to understand the evolution and the process the Perau Formation polymetallic-sulfide deposits were submitted.

5.1. Sulfide mineral chemistry

Sphalerite has been considered the most refractory sulfide, potentially recording evidence for the conditions of its genesis (Grammatikopoulos *et al*., 2006). The iron content in the sphalerite in equilibrium with pyrite is known to depend on both temperature and fugacity of sulfur (Demir *et al.*, 2013). The difference in Fe content between barite-rich ore and silica-rich ore in the Perau mine can be interpreted as differences in temperature during the ore formation of these different levels of mineralization. In the case of Perau mine, the barite-rich ore is formed at a low temperature than the silica-rich ore, once the barite-rich ore shows lower contents of Fe (avg. 1.22 wt.%) than the silica-rich ore (avg.7.24 wt.%.)

Several studies (Gavelin and Gabrielson, 1947; Loftus Hills and Solomon, 1967; Seccombe, 1977; Bralia *et al*., 1979; Green *et al*., 1981; Campbell and Ethier, 1984; Bajwah *et al*., 1987; Ghorbani *et al*. 2019) have employed the Co-Ni contents and Co/Ni ratio of pyrite in sulfide deposits to discriminate between submarine exhalative, magmatic or sedimentary origins for ore deposits. According to the authors, volcanogenic pyrite has Co contents between 400-2400 ppm and Co/Ni ratios above 5-10, higher than those typicall of sedimentary (< 100 ppm cobalt an Co/Ni value of < 1)or hydrothermal-related pyrites (Co/Ni: 1–5). Based on their Co content and Co/Ni ratio, the Perau and Canoas mineralizations show characteristic distinct behaviors (Fig. 14). Pyrite from the Perau deposit shows Co/Ni ratios in the range of 0.19 to 5.16, suggesting a sedimentary or hydrothermal origin. However, high cobalt values suggest a magmatic origin when plotted in the diagram of Brill (1989) and Bajwah *et al*. (1987) (Fig. 14). The Co/Ni ratios in pyrite from the Canoas deposit varies from 32.96 to 110.15 and are plotted in the field of volcano-exhalative origin (Fig. 14).

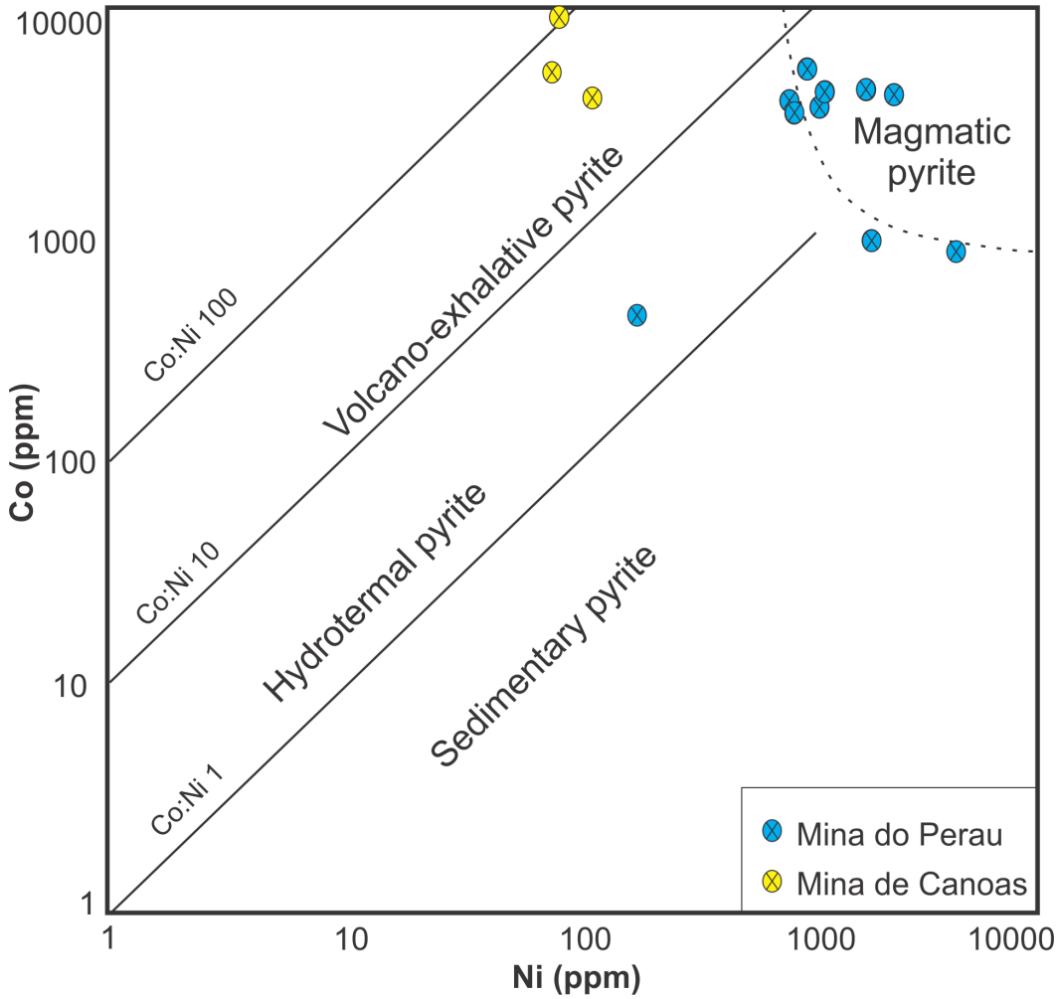

Fig. 14. The plot of the Co and Ni contents of pyrite from Perau and Canoas deposits. Fields of pyrite in the various origins, after Brill (1989) and Bajwah *et al.* (1987), are shown for comparison.

5.2. Sulfur Source

The composition of sulfur isotope varies in different types of deposits, and it is indicative of the sulfur sources and the mechanisms of ore precipitation (Ohmoto and Rye, 1979). The sulfur isotope values range from -8 to +30 ‰ in SEDEX deposits (Leach *et al*., 2005), from 0 to +4 ‰ in Broken Hill-type deposits (Parr and Plimer, 1993), and are dominantly negative in Mississipi Valley Type (MVT) deposits (Wilkinson, 2013). This behavior is explained as related with a variety of crustal sources and different mechanism of reduction (BSR - bacteriogenic sulfate reduction; TSR - thermochemical sulfate reduction) that acted in the formation of each type of deposit.

According to Daitx (1996), the low S-isotope values obtained in sulfides in the Canoas deposit (+1.2 to +8.2 ‰) indicate its formation from hydrothermal fluids containing sulfur of magmatic origin, either from basic magmas or from leaching of

magmatic sulfides in crustal rocks. According to the author it doesn't suggest a pattern similar to that exhibited by most SEDEX type deposits. However, the data presented here for the Canoas deposit shows enrichment in the heavy isotopes of sulfur, with values of $\delta^{34}S$ from +4.6 to +13.16 ‰. The S-isotope data obtained in this work for sulfides of Perau deposit range from -1.88 to +3.25‰. The low S-isotope values for the Canoas and Perau deposits could be explained as a magmatic origin for the sulfur. However, many Proterozoic SEDEX-type deposits display a significant variation in the $\delta^{34}S$ values (Fig.15). In the case of SEDEX deposits, the sulfur content is believed to be ultimately derived from seawater sulfate (Wilkinson, 2013). According to the author, evidence for a seawater origin is provided by the parallel evolution of the isotopic composition of deposit sulfides and the secular seawater sulfate and sedimentary pyrite curves in the Phanerozoic. Kiyosy and Krouse (1990) admit that deposit sulfides have $\delta^{34}S$ between contemporaneous seawater sulfate and seawater, probably the range of sulfide produced by TSR at around 150°C. For Lyons *et al*. (2006), high hates of BSR in basins with restricted sulfate replenishment could be another explanation for this range of values. In both cases, the sulfate involved in the formation of SEDEX deposits is derived from connate brines or sulfate minerals from the host rocks or contemporaneous seawater circulation (Wilkinson, 2013). The Proterozoic marine sulfur record is less restricted, and there is much more overlap between BSR and TSR, making it challenging to identify the mechanisms that occured (Wilkinson, 2013). For the Perau Formation deposits, we interpret that reduced seawater sulfate is the primary source of sulfur with the sulfide produced by BSR and/or TSR. The values of S-isotope bellow the sedimentary pyrite average at the time of ore formation suggest these deposits contain significant bacteriogenic sulfide (e.g., Sullivan, and HYC). The $\delta^{34}S$ values between 20.6 and +22.2 ‰ in barite indicate seawater dominated fluids as expected by the curves of the secular seawater sulfate (Fig. 15).

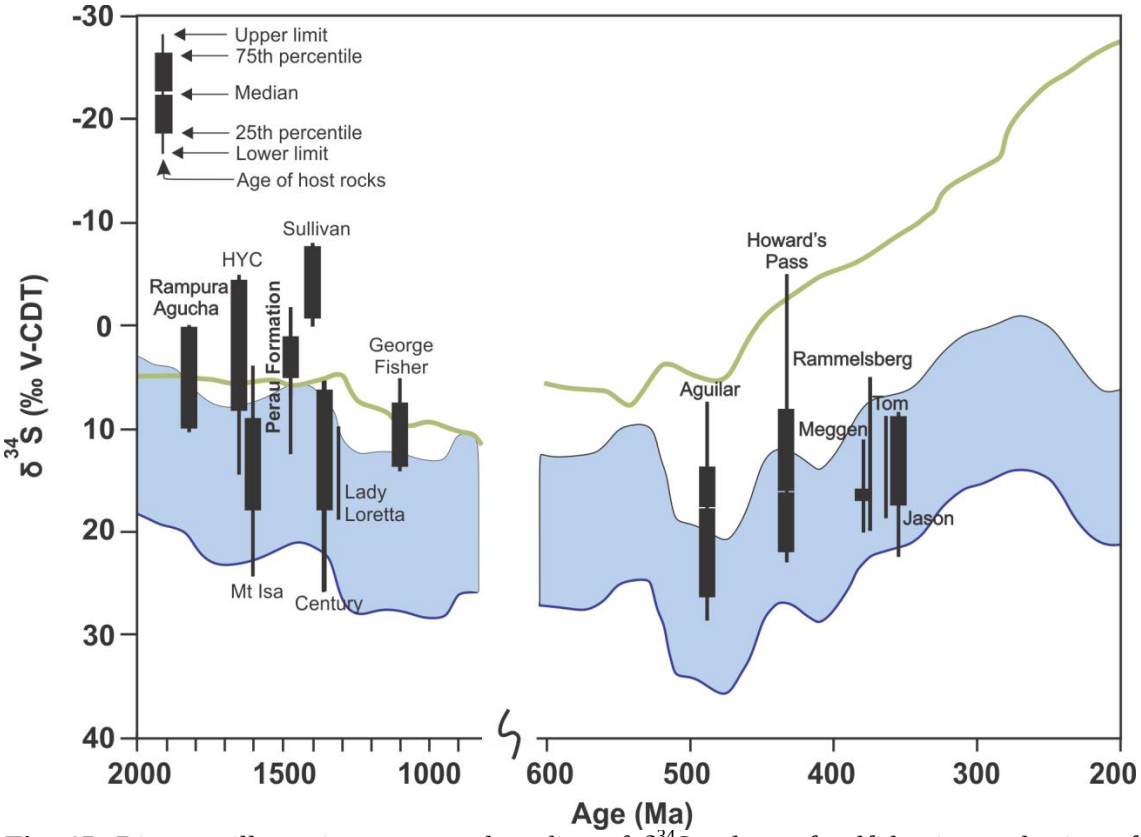

Fig. 15. Diagram illustrating range and median of $\delta^{34}S$ values of sulfides in a selection of SEDEX deposits and the Perau Formation deposits (n=18) plotted at their approximate host-rock/ formation age compared with marine sulfate composition (blue line) and average composition of sedimentary pyrite (olive line) as produced by BSR. The blue-shaded field indicates the likely range of sulfide compositions produced by TSR of seawater-derived sulfate at 150 C (Kiyosu and Krouse, 1990). The correspondence between deposit compositions and marine sulfate evolution supports a marine sulfate origin for ore sulfides, reduced by TSR and/or BSR. Data compiled in Leach *et al*. (2005). Sulfur isotope curves from Farquhar *et al*. (2010). Modified from Wilkinson (2013).

5.3. Fluid inclusion constraints on the mineralization

The analysis of FIA-01 (primary) fluid inclusions hosted in quartz-rich samples from the Perau and Canoas Pb-Zn-Ag-(Cu-Ba) mineralizations shows the coexistence of aqueous-carbonic, carbonic-rich, and aqueous inclusions in the same assemblage. Variations in the CO_2/H_2O ratios, observed in type 2 aqueous-carbonic fluid inclusions, associated with the fact that the final homogenization occurs both in the liquid and the vapor phases at the same temperature range (Fig. 13f) are indicators of unmixing of initially homogeneous fluid (Ramboz *et al.*, 1982). In other hand, variations in CO_2/H_2O ratios could also be explained by post-entrapment selective leakage of water from a homogeneous parental fluid during the crystal-plastic deformation (e.g., Crawford and Hollister, 1986; Bakker and Jansen, 1990; Hollister, 1990; Johnson and Hollister, 1995; Faleiros *et al.*, 2010).

To test the hypothesis of fluid inclusions produced by phase separation (immiscibility, unmixing) or by post-entrapment modifications the use plots of CO_2 volumetric ratio (V_{CO2}) against density and salinity (e.g., Faleiros *et al.*, 2014) can be employed. As a result, water-rich aqueous-carbonic inclusions produced by phase separation must show lower densities when compared to water-poor inclusions. The opposite case indicates the inclusions are formed by selective water loss (leakage).

The V_{CO2} versus CO_2 density plot of the FIA-01 aqueous-carbonic inclusions shows a fluctuation of CO_2-rich phase density from 0.76 to 0.85 g/cm³ without co-variance with the V_{CO2} values (Fig. 16a). The V_{CO2} versus salinity plot does not show a correlation with strain-induced water loss, once the leakage process leads to an increase in the salinity values (Fig. 16b; e.g., Johnson and Hollister, 1995).

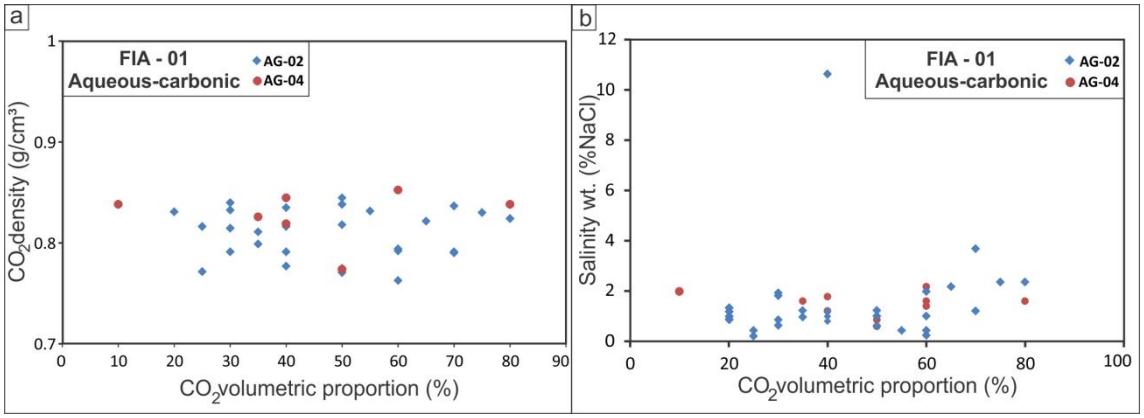

Fig. 16. (a) The plot of CO_2 volumetric proportion versus CO2 density; (b) The plot of VCO2 versus salinity %wt. (NaCl) for FIA-1 inclusions.

In the case of fluid immiscibility has operated as the main mechanism, three general criteria must be satisfied (Ramboz et al., 1982). *(i) The different type inclusions must occur in the same regions of the same sample, and there must be good evidence of their contemporaneous trapping; (ii) The different inclusion types must homogenize within the same range of temperature (because trapping is not an instantaneous and strictly isothermal--isobaric process) by opposite modes (into the liquid and vapor phase), reflecting contrasting densities; and (iii) The bulk molar volumes of lower and higher density phase-rich fluid inclusions types must be compatible with equilibrium coexistence at a unique value of Th. As a consequence, if one inclusion type decrepitates before homogenizing, the other type must behave equivalently, if they are similar in size and shape.*

The three types of fluid inclusions described in the FIA-1 occur in the same regions of the samples (Fig. 12a), which is evidence for coeval trapping. The homogenization for liquid and vapor of FIA-1 (Fig. 13f) are in the same range of temperatures. Only a few inclusions of the three types have decrepitated, at the same range of temperature, during heating stages, and must of all show similar size and shape.

In the bases of petrographic characteristics and microthermometric behavior observed in FIA-01 fluid inclusions and on the tests accomplished above, we concluded that FIA-01 primary fluid inclusions represent immiscible fluids (aqueous-carbonic, carbonic, and aqueous) derived from unmixing of homogeneous parental fluid, in which the nearly pure CO_2 and H_2O-NaCl-$MgCl_2$ represents the end-members of the phase separation.

The analysis of FIA-02 and FIA-03 secondary fluid inclusions hosted in quartz levels of silica-rich ore in the Canoas mine mineralization (Fig. 8f) shows the presence of aqueous and carbonic inclusions in different fluid inclusions assemblages. The eutectic temperatures of fluid inclusions of FIA-03 range between -59.2 to -67.5 °C (mean: ±63.7), indicating that the aqueous system might contain H_2O-NaCl-$CaCl_2$ (Fig. 17a). The significant deviation of the stable eutectic value (-52 ºC) may indicate the presence of other dissolved salts or metastability typical of the H_2O-NaCl-$CaCl_2$ system (e.g., Goldstein and Reynolds, 1994).

Bivariate plot of salinity against homogenization temperature (Th) from aqueous fluids (FIA-03) was used to evaluate the processes involved during their evolution. The plot FIA-03 aqueous inclusions shows a strong variation of salinity for relatively

constant values of Th (Fig. 17b), which can be explained by the mixing between fluids of different salinities or different fluid-rock interactions.

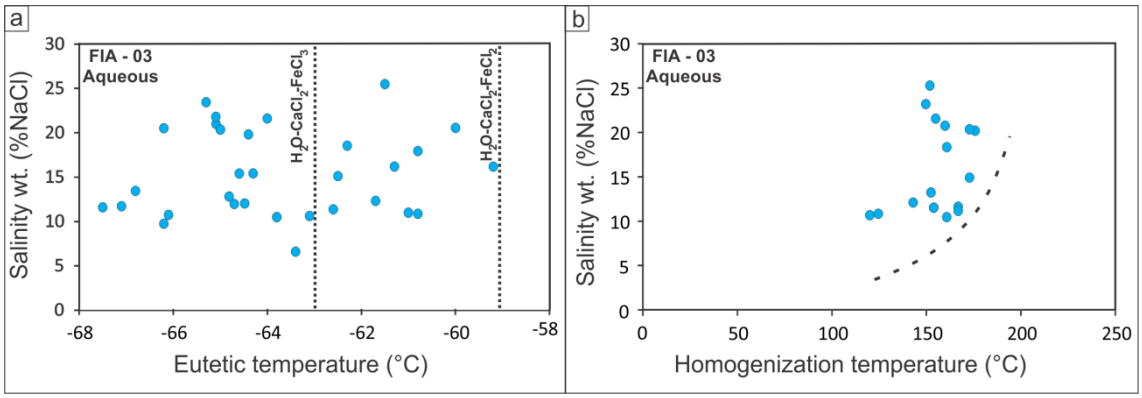

Fig. 17. (a) The plot of eutectic temperature versus salinity; (b) The plot of homogenization temperature versos salinity %wt. (NaCl) for FIA-3 inclusions.

For Rich (1979), metamorphic fluids spread a wide range of salinity and temperature. In most cases, the salinity of the fluids is low to moderate, with an exception in cases where an evaporitic unit is a part of the sequence of rocks that was metamorphosed. Touret (1977), in turn, characterizes metamorphic fluids based on volatile composition.

According to the definitions of metamorphic fluids and the metamorphic conditions that Perau formation was subjected, we interpret that the fluid inclusion data obtained in this work indicate that the primary and secondary fluid inclusions from Canoas e Perau deposits originate from metamorphic fluids. Although high salinities are not common in metamorphic fluids, we interpreted that the high salinities observed could reflect the original high salinity of hydrothermal fluids acting during the formation of the mineralized Pb-Zn-Ag-(Cu-Ba) deposits hosted by Perau Formation

The compositions of the fluids, with chloride complexes, might be responsible for transportation and reprecipitation of the base metals during the metamorphism of the Perau and Canoas deposits.

The plots of FIA-01 and FIA-03 salinity versus temperature show the FIA 01 inclusions present metamorphic-type and VMS-type fluid signatures, while FIA-03 are plotted in the MVT fluid field (Fig 18). The plots are similar to the plots of the study of fluid inclusion in sin-tectonic quartz veins of the Perau Formation, obtained by Fedalto (2018). However, primary fluid inclusions in this study show lower salinities than those obtained by Fedalto (2018). The classification of the Perau and Canoas deposits in SEDEX or CD host Pb-Zn types attributed for many authors (Barbour and Oliveira,

1979; Daitx, 1996; Dardenne and Schobbenhaus, 2001) fit better all the features described for these deposits in this work and previous works.

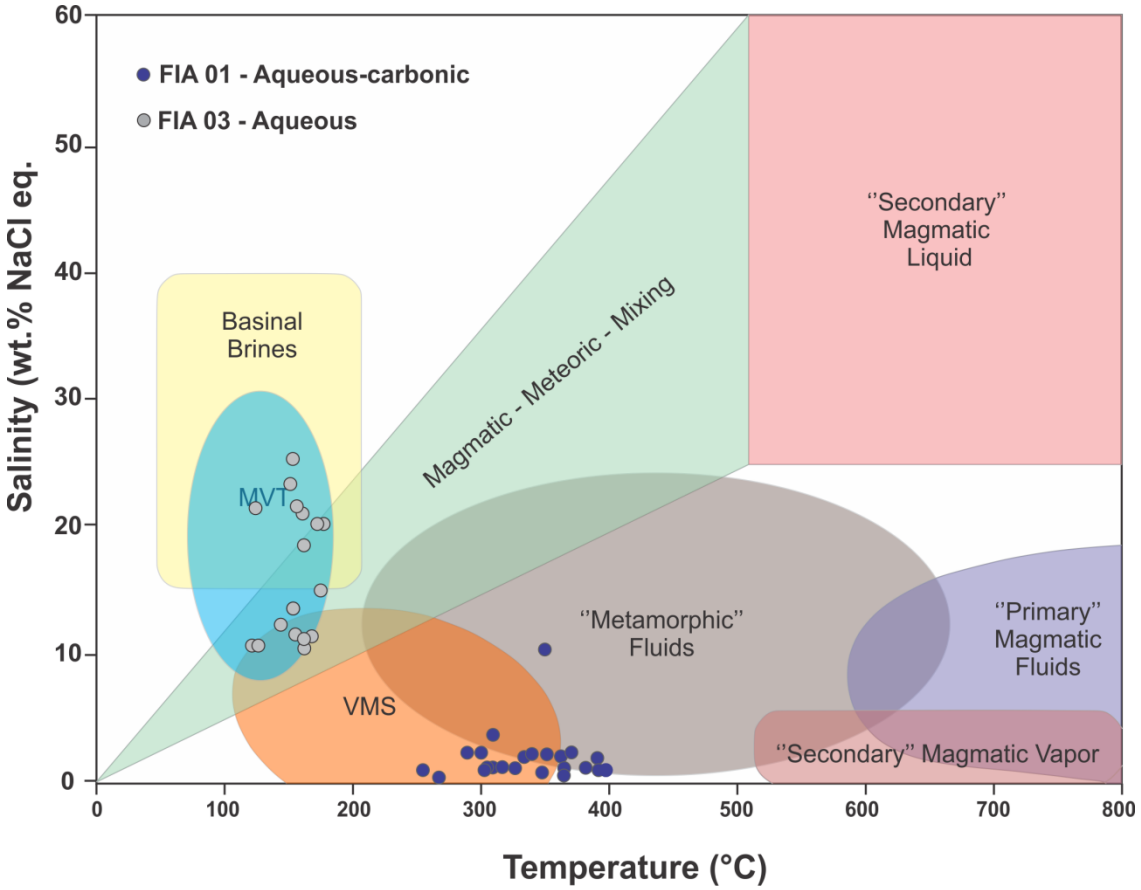

Fig. 18. The plot of temperature versus salinity showing the distribution of hydrothermal solutions of different origins (Bodnar 1999), within Perau and Canoas deposits fluid inclusion data.

6. CONCLUSIONS

The data obtained in this study, suggest that the evolution of mineralizations hosted by Perau Formation evolved at least two stages.

(1) Pb-Zn-Ag (Cu-Ba) primary mineralization (SEDEX or CD-host deposits) shown by the sulfur isotope compositions obtained in Perau and Canoas deposits (-1.88 to +3.25‰, and +1.2 to +13.16 ‰, respectively), which have similarity with other Proterozoic SEDEX deposits distributed worldwide (Fig. 15). The primary source of sulfur is the reduced seawater sulfate produced by Bacterial Sulfate Reduction (BSR) and Thermochemical Sulfate Reduction (TSR) mechanisms. S-isotope values in barites of ore zone range between 20.6 and +22.2 ‰, indicating seawater-dominated fluids as expected by the curves of the secular seawater sulfate. The temperature obtained by sphalerite-galena pair yielded values of 227ºC, which is in the same range of typical SEDEX mineralizations (e.g., Emsbo, 2009). The differences in Fe content in sphalerite from barite-rich and silica-rich ores show these two ore zones have been formed in distinct temperatures, with the barite-rich ore formed in lower temperatures than the silica-rich ore. Co/Ni ratios in pyrites from the Perau and Canoas deposits are plotted in volcano-exhalative, sedimentary or hydrothermal, and magmatic fields, not being a useful discriminate tool in the case of Perau Formation deposits.

(2) Modifications (remobilization and reconcentration) of the Pb-Zn-Ag (Cu-Ba) mineralization due to deformation and metamorphism in greenschist to amphibolite facies, during the Brasiliano orogeny. Fluid inclusion data obtained in this work suggest the metamorphic fluids, represented by FIA-01 primary fluid inclusions (aqueous-carbonic, carbonic and aqueous) constituted by immiscible fluids derived from unmixing of a H_2O-NaCl-$MgCl_2$-CO_2 fluid, and FIA-03 secondary aqueous fluid inclusions which represent the H_2O-NaCl-$CaCl_2$ system, both composed of chloride complexes, may have played a hole in the reconcentration and remobilization of base metals.

7. REFERENCES

Addas, W. & Vinha, C. A. G. da. Projeto Sudelpa: relatório final reconhecimento geoquímico (parte 1 a 3). São Paulo: Sudelpa/CPRM, 1975. 136 p.

Alegri, V.; Pizzato, L. G.; Ferrari, C. P.; Addas, W.; Morgental, L. A. Projeto Serra do Jabaquara: relatório de prospecção preliminar. São Paulo: CPRM, 1980.

Almeida F.F.M. 1967. Origem e evolução da plataforma brasileira. Rio de Janeiro, DNPM-DGM, Boletim, 241, 36p.

Almeida, F. F. M. de; Amaral, G.; Cordani, U.G.; Kawashita, K. The Precambrian evolution of the South American cratonic margin south of the Amazonas river. In: NAIRN, A. E. M.; STILLE, F. G. (Ed.). The ocean basin and margins. New York: Plenum, 1973. V. 1, p. 411-446.

Almeida, F.F.M. de; Hasui, Y.; Brito Neves, B.B.; Fuck, R.A. Províncias estruturais brasileiras. In: SIMPÓSIO DE GEOLOGIA DO NORDESTE, 8., Campina Grande. Atas… Campina Grande: SBG, 1977. 499 p. (Boletim do Núcleo Nordeste da SBG, 6). p. 363-391.

Almeida, F.F.M. de; Hasui, Y.; Brito Neves, B.B.; Fuck, R.A. Brasilian structural provinces: an introduction. Earth Science Review, Amsterdam, v. 17, n. 1, p. 1-29, 1981.

Archer, D.G., 1992, Thermodynamic Properties of the NaCl + H2O System. II. Thermodynamic Properties of NaCl (aq), NaCl2H2O (cr), and Phase Equilibria: J. Phys. and Chem. Ref. Data, v. 21, p. 793-829, DOI:10.1056.

Bajwah, Z.U., Seccombe, P.K., Offler, R., 1987. Trace element distribution; Co: Ni ratios and genesis of the Big Cadia iron–copper deposit, New South Wales, Australia. Mineral. Deposita 22, 292–300.

Bakker, R.J., 1997, Clathrates: Computer programs to calculate fluid inclusion V-X properties using clathrate melting temperatures: Computers and Geosciences, v. 23, p. 1-18, DOI:10.1016/S0098-3004(96)00073-8.

Bakker, R.J., 2003, Package FLUIDS 1. Computer programs for analysis of fluid inclusion data and for modelling bulk fluid properties: Chemical Geology, v. 194, p. 3-23.

Bakker, R.J., and Jansen, B.H., 1990, Preferential water leakage from fluid inclusions by means of mobile dislocations: Letters to Nature, v. 345, p. 58-60.

Barbour, A. P., Oliveira, M. A. F. 1979. Pb, Zn, Cu e Ba do Distrito Perau – modelo sedimentar para sulfetos do Vale do Ribeira. Boletim IG – USP. 10:97-120.

Barbour, A. P.; Brito Neves, B. B.; Medeiros, R. A. Algumas implicações tectônicas na gênese das mineralizações sulfetadas do tipo Panelas no Vale do Ribeira, SP-PR. Revista Brasileira de Geociências, v.20, n.1-4, p.46-54, 1990.

Basei, M. A. S.; Siga Junior, O.; Kaulfuss, G. A.; Cordeiro, H.; Nutman, A.; Sato, K.; Cury, L. F.; Prazeres Filho, H. J.; Passarelli, C. R.; Harara, O. M.; Reis Neto, J. M.; Weber, W. 2003. Geochronology and isotope geochemistry of Votuverava and Perau

Mesoproterozoic basins, Southern Ribeira Belt, Brazil. In: South American Symposium on Isotope Geology, Salvador. p. 501-504.

Bettencourt, J. S; Daitx, E. C.; Moreira, M. Z.; Matsui, E. (1992). Estudo isotópico pelos métodos $^{13}C/^{12}C$, $^{18}O/^{16}O$, dD e $^{34}S/^{32}S$ dos depósitos de chumbo-zinca-prata do Vale do Ribeira, Estados de São Paulo e Paraná. FAPESP, Processo n° 90/2139-2, 47p.

Bigarella, J. J.; Salamuni, R. 1958a. Contribuição à geologia da região sul da Série Açungui (Estado do Paraná). Boletim Paulista de Geografia, São Paulo 29, 1-14.

Bodnar, R.J.(1999) Hydrothermal Solutions. in Encyclopedia of Geochemistry, C.P. Marshall and Fairbridge eds., Kluwer Academic Publishers, Lancaster, pp. 333-337.

Borin Júnior, T.; Pinto, G. G.; Silva, A, A. A. G. P. da; Morgental, A.; Castro, V. H. S. de. 1980. Mineralizações filoneanas polimetálicas contendo ouro e prata associados a metais básicos descobertos pelo Projeto Eldorado, Vale do Ribeira (SP). In.: CONGRESSO BRASILEIRO DE GEOLOGIA, 31, Camboriú, 1980. Anais. Camboriú: SBG, 1980, v. 3, p. 1444-1458.

Borin Júnior, T. Projeto Pilões: relatório de prospecção preliminar. São Paulo: CPRM. 1983

Bralia, A., Sabatini, G., Troja, F., 1979. A revaluation of the Co/Ni ratio in pyrite as a geochemical tool in ore genesis problems. Evidences from southern Tuscany pyritic deposits. Miner. Deposita 14, 353–374.

Brill, B.A., 1989. Trace-element contents and partitioning of elements in ore mineral from the CSA Cu-Pb-Zn deposit, Australia. Can. Mineral. 27, 263–274.

Brito Neves, B.B.; Campos Neto, M.C.; Fuck, A.F. 1999. From Rodinia to Western Gondwana: an approach to the Brasiliano-Pan African Cycle and orogenic collage. Episodes, 22:155-166.

Campanha, G.A.C. 1991. Tectônica proterozóica no Alto e Médio Vale do Ribeira, Estados de São Paulo e Paraná. São Paulo. Tese de doutoramento. Instituto de Geociências Universidade de São Paulo. 296 p, anexos.

Campanha, G.A.C. and Sadowski, G.R., 1999. Tectonics of the Southern Portion of the Ribeira Belt (Apiaí Domain). Precambrian Research, 98 (1): 31-51.

Campanha, G.A.C. and Brito Neves, B.B. 2004. Frontal and oblique tectonics in the Brazilian shield. Episodes, 27(4): 255-259.

Campanha, G. A. C., Faleiros, F. M. Neoproterozoic terrane collage in the southern and central Ribeira Belt, Brazil. In: INTERNATIONAL GONDWANA SYMPOSIUM, 12., 2005, Mendoza. Gondwana 12 conference: geological and biological heritage of Gondwana. Mendoza: Academia Nacional de Ciências, 2005, v. 1, p. 81.

Campanha, G.A. C., Faleiros, F. M., Basei, M., Tassinari, C. G. Nutman, A., Vasconcelos, P. (2015). Geochemistry and age of mafic rocks from the Votuverava Group, southern Ribeira Belt, Brazil: Evidence for 1490Ma oceanic back-arc magmatism. Precambrian Research. 266. 10.1016/j.precamres.2015.05.026.

Campanha, G.A. C., Basei, M., Faleiros, F. M., Nutman, A. (2016). The Mesoproterozoic to Early Neoproterozoic passive margin Lajeado Group and Apiaí Gabbro, Southeastern Brazil. Geoscience Frontiers. 7. 683 - 694. 10.1016/j.gsf.2015.08.004.

Campbell, F.A., Ethier, V.G., 1984. Nickel and cobalt in pyrrhotite and pyrite from the Faro and Sullivan orebodies. Can. Mineral. 22, 503–506.

Crawford, M.L., and Hollister, S., 1986, Metamorphic fluids: the evidence from fluid inclusions: Fluid-rock interactions during metamorphism. Advances in Physical Geochemistry, p. 1-35, DOI:10.1007/978-1-4612-4896-5_1.

Cury, L.F.; Kaulfuss, G.A.; Siga Junior, O.; Basei, M.A.S.; Harara, O.M.; Sati, K. Idades U-Pb (zircões) de 1.75 Ga em granitoides alcalinos deformados dos núcleos Betara e Tigre: evidências de regimes extensionais do Estateriano na faixa Apiaí. Geol. USP, Sér. cient., São Paulo, v. 2, p. 95-108, 2002.

Daitx, E. C. *et al*., 1983. Projeto Anta Gorda – Fases III. CPRM.

Daitx, E. C. 1984. Projeto Anta Gorda – Fase IV. CPRM.

Daitx, E.C. Origem e evolução dos depósitos sulfetados tipo Perau (Pb-Zn-Ag), com base nas jazidas Canoas e Perau (Vale do Ribeira, PR). 1996. 453 f. Tese (Doutorado) – Instituto de Geociências e Ciências Exatas, Universidade Estadual Paulista Júlio de Mesquita, Rio Claro, 1996.

Dardenne, M.A.; Schobbenhaus, C. Metalogênese do Brasil. Brasília: EDUnB, 2001. v. 1.

Delgado, I. M.; Souza, J. D.; Silva, L. C.; Silveira Filho, N. C.; Santos, R. A.; Pesdreira, A. J.; Guimarães, T.; Angelin, L. A. A.; Vasconcelos, A. M.; Gomes, I. P.; Lacerda Filho, J. V.; Valente, C. R.; Perrotta, M.; Heineck, C. A. Geotectônica do Escudo Atlântico. In: BIZZI, L. A. *et al*. Geologia, tectônica e recursos minerais do Brasil: texto, mapas e SIG.Brasilia: CPRM, 2003. P. 227–234.

Demir, Yılmaz & Uysal, İbrahim & Sadıklar, M.B. (2013). Mineral chemical investigation on sulfide mineralization of the Istala deposit, Gümüşhane, NE-Turkey. Ore Geology Reviews. 53. 306–317. 10.1016/j.oregeorev.2013.01.014.

Duan, Z., Moller, N., and Weare, J.H., 1992a, An equation of state for the CH4-CO2-H2O system: II. Mixtures from 50 to 1000ºC and 0 to 1000 bar: Geochimica et Cosmochimica Acta, v. 56, p. 2619-2631.

Duan, Z., Møller, N., and Weare, J.H., 1992b, An equation of state for the CH4-CO2-H2O system: I. Pure systems from 0 to 1000ºC and 0 to 8000 bar: Geochimica et Cosmochimica Acta, v. 56, p. 2605–2617, DOI:10.1016/0016-7037(92)90347-L.

Duschek, W., Kleinrahm, R., and Wagner, W., 1990, Measurement and correlation of the (pressure, density, temperature) relation of carbon dioxide. The homogeneous gas and liquid regions in the temperature range from 217 K to 340 at pressures up to 9 MPa: J. Chem. Thermodynamics, v. 22, p. 827-840.

Emsbo, Poul, 2009, Geologic criteria for the assessment of sedimentary exhalative (SEDEX) Zn-Pb-Ag deposits: U.S. Geological Survey Open-File Report 2009−1209, 21 p.

Faleiros, A.M., Campanha, G.A.C., Faleiros, F.M., and Bello, R.M.S., 2014, Fluid regimes, fault-valve behavior, and formation of gold-quartz veins - The Morro do Ouro Mine, Ribeira Belt, Brazil: Ore Geology Reviews, v. 56, p. 442-456, DOI:10.1016/j.oregeorev.2013.05.002.

Faleiros, F.M. Evolução de terrenos tectonometamórficos da Serrania do Ribeira e Planalto Alto Turvo (SP, PR). 2008. 306 p. Tese (Doutorado em Geoquímica e Geotectônica) – Universidade de São Paulo, São Paulo, São Paulo, 2008.

Faleiros, F.M.; Campanha, G. A. C; Bello, R. M. S. Quartz recrystallization regimes, c-axis texture transitions and fluid inclusion reequilibration in a prograde greenschist to amphibolite facies mylonite zone (Ribeira Shear Zone, SE Brazil). Tectonophysics, v. 485, p. 193-214, 2010.

Faleiros, F.M., Campanha, G.A.C., Martins, L., Vlach, S.R.F., and Vasconcelos, P.M., 2011. Ediacaran high-pressure collision metamorphism and tectonics of the southern Ribeira Belt (SE Brazil): Evidence for terrane accretion and dispersion during Gondwana assembly: Precambrian Research, v. 189, p. 263-291.

Faleiros, Frederico Meira; Morais, Silvia Maria; Costa, Vicente Sérgio. Geologia e recursos minerais da folha Apiaí SG.22-X-B-V: escala 1:100.000: estados de São Paulo e Paraná. São Paulo: CPRM, 2012.

Faleiros, Frederico & Silva, Mauricio. (2013). Geologia e recursos minerais da folha Eldorado Paulista – SG.22-X-B-VI, estado de São Paulo, Escala 1:100.000.

Faleiros, F.M., Campanha, G.A.C., Pavan, M., Almeida, V. V., Rodrigues, S.W.O., and Araújo, B.P., 2016, Short-lived polyphase deformation during crustal thickening and exhumation of a collisional orogen (Ribeira Belt, Brazil): Journal of Structural Geology, v. 93, p. 106-130.

Farquhar J, Wu NP, Canfield DE, and Oduro H (2010) Connections between sulfur cycle evolution, sulfur isotopes, sediments, and base metal VMS, SEDEX, and MVT deposits. Economic Geology 105: 509–533.

Fedalto, G. Caracterização petrotectônica da Formação Perau: Implicação para as mineralizações de Pb-Zn (Cu-Ba). Curitiba, 2018 Dissertação de mestrado. Universidade Federal do Paraná.

Fleischer, R. A pesquisa de chumbo no Brasil. In: CONGRESSO BRASILEIRO DE GEOLOGIA, 29., Ouro Preto, 1976. Anais. Ouro Preto: Sociedade Brasileira de Geologia, 1976. v. 1. p. 19-32.

Fritzson, JR, O., Piekarz, G. F. 1982. Geologia e Potencial Econômico do Grupo Setuva, Paraná. Anais do XXXII Congresso Brasileiro de Geologia, Salvador, Bahia, 1982, V.3. 987-1000.

Fuck, R.A.; Brito Neves, B.B.; Schobbenhaus, C. Rodinia descendants in South America. Precambrian Research, Amsterdam, v. 160, p. 108-126, 2008.

Gavelin, S., Gabrielson, O., 1947. Spectrochemical investigation of sulfide minerals from ores of the Skellefte district. The significance of minor constituents for certain practical and theoretical problems of economic geology. Sver. Geol. Undersokn. Ser. C 491, Arsbok 41, (10).

Ghorbani, Mahsa & Hosseinzadeh, Mohammad Reza & Moayyed, Mohsen & Maghfouri, Sajjad. (2019). Metallogenesis of Precambrian SEDEX-type Barite-(Pb-Cu-Zn) deposits in the Mishu mountain, NW Iran: Constrains on the geochemistry and tectonic evolution of mineralization. Ore Geology Reviews. 10.1016/j.oregeorev.2019.02.024.

Goldstein, R.H., and Reynolds, T.J., 1994, Systematics of fluid inclusions in diagenetic minerals: SEPM short course 31, v. 31, 199 p.

Goodfellow, W.D., Lyndon J.W., Turner R.J.W. 1993. Geology and Genesis of Stratiform Sediment Hosted (SEDEX) Zinc-Lead-Silver Sulphide Deposits. In Kirkham, R.V.; Sinclair, W.D.; Thorpe, R.I. and Duke, J.M.(eds.), Mineral Deposits Modeling: Geological Association of Canada, Canadá, Special Paper 40: 201-251.

Goodfellow, W.D.; Lydon, J.W. Sedimentary exhalative (SEDEX) deposits. 2007. In: Goodfellow, W.D. (ed.) Mineral deposits of Canada—A synthesis of major deposit-types, district metallogeny, the evolution of geological provinces, and exploration methods. Geological Association of Canada, p. 163–184.

Grammatikopoulos, T.A., Valeyev, O., Roth, T., 2006. Compositional variation in Hg-bearing sphalerite from the polymetallic Eskay Creek deposit, British Columbia, Canada. Chem. Erde 66, 307–314.

Green, G.R., Solomon, M., Walshe, J.L., 1981. The formation of the volcanic-hosted massive sulfide ore deposit at Rosebery, Tasmania. Econ. Geol. 76, 304–338.

Hasui, Y.; Sadowski, G.R. Evolução geológica do Pré-Cambriano na região sudeste do Estado de São Paulo. Boletim IG USP, v. 6, p.180 - 200, 1976.

Heilbron, M.; Machado, N. Timing of terrane accretion in the Neoproterozoic–Eopaleozoic Ribeira belt, SE Brazil. Precambrian Research, v. 125, n.1-2,p. 87–112, jul. 2003.

Heilbron, M.; Machado, N.; Simonetti, T.; Duarte, B. 2003. A Palaeoproterozoic orogen reworked within the Neoproterozoic Ribeira belt, SE Brazil. In: South American Symposium on Isotope Geology, 4, Short Papers, p. 186-189.

Heilbron, M.; Mohriak, W.; Valeriano, C.M.; Milani, E.J.; Almeida, J.; TUPINAMBÁ, M. From Collision to Extension: The Roots of the Southeastern Continental margin of Brazil. In: MOHRIAK, W.; TALWANI, M. (Ed.). Atlantic Rifts and Continental Margins.Washington, DC: American Geophysical Union, 2000. P.1-32 (Geophysical Monograph Series, 115) DOI: 10.1029/GM115.

Heilbron, M.; Valeriano, C. M.; Tassinari, C. C. G.; Almeida, J. C. H.; Tupinamba, M.; Siga Junior, O.; Trouw, R. A. J. Correlation of Neoproterozoic terranes between Ribeira Belt, SE Brazil and its African counterpart: comparative tectonic evolution and open questions. Special Publications, v. 294, p. 211-237, Jan. 2008. https://doi.org/10.1144/SP294.12

Hollister, L.S., 1990, Enrichment of CO2 in fluid inclusions in quartz by removal of H2O during crystal-plastic deformation: Journal of Structural Geology, v. 12, p. 895-

Johnson, E.L., and Hollister, L.S., 1995, Syndeformational fluid trapping in quartz: determining the pressure- temperature conditions of deformation from fluid inclusions and the formation of pure CO2 fluid inclusions during grain- boundary migration: Journal of Metamorphic Geology, v. 13, p. 239-249, DOI:10.1111/j.1525-1314.1995.tb00216.x.

Kiyosu Y and Krouse HR (1990) The role of organic acid in the abiogenic reduction of sulfate and the sulfur isotope effect. Geochemical Journal 24: 21–27.

Large, R., McGoldrick, P., Bull, S., and Cooke, D., 2004, Proterozoic stratiform sediment-hosted zinc-lead-silver deposits of northern Australia, in Deb, M., and Goodfellow, W.D., eds., Sediment hosted lead-zinc sulphide deposits; attributes and models of some major deposits in India, Australia and Canada: New Delhi, Narosa Publishing House, p. 1–23.

Leach, D.L., Sangster, D.F. Kelley, K. D., Large, R. R., Garven, G., Allen, C. R., Gutzmer, J., and Walters, S., 2005, Sediment-hosted lead-zinc deposits: A global perspective: ECONOMIC GEOLOGY 100TH ANNIVERSARY VOLUME, p. 561−608.

Lyons TW, Gellatly AM, McGoldrick PJ, and Kah LC (2006) Proterozoic sedimentary exhalative (SEDEX) deposits and links to evolving global ocean chemistry. In: Kesler SE and Ohmoto H (eds.) Evolution of Early Earth's Atmosphere, Hydrosphere, and Biosphere – Constraints from Ore Deposits, GSA Memoirs 198, pp. 169–184. Boulder, CO: Geological Society of America.

Loftus Hills, G.D., Solomon, M., 1967. Cobalt, nickel and selenium in sulphides as indicators of ore genesis. Miner. Deposita 2, 228–242.

Lydon, J.W., 1996, Sedimentary exhalative sulphides (SEDEX), in Eckstrand, O.R., Sinclair, W.D., and Thorpe, R.I., eds., Geology of Canadian mineral deposit types: Geological Survey of Canada, Geology of Canada, v. 8, p. 130–152.

Lopes Júnior, I.; Câmara, M. M.; Vasconcelos, C. S. de; Pizzatto, L. G. A prospecção geoquímica descobrindo novas mineralizações auríferas no Vale do Ribeira. In: CONGRESSO BRASILEIRO DE GEOLOGIA, 38., Camboriú, 1994. Anais. Camboriú: SBG, 1994. p. 170-171.

Macedo, A. B.; Addas, W.; Batolla Júnior, F. Metodologia de prospecção geoquímica em Minas do Vale do Ribeira (PR). In: SIMPÓSIO REGIONAL DE GEOLOGIA, 3., 1981, Curitiba. Atas. Curitiba: SBG, 1981. p. 71-81.

Maniesi, V. Petrologia das rochas anfibolíticas das regiões de Adrianópolis, Campo Largo e Rio Branco do Sul/ PR. 1997. 215 f. Tese (Doutorado) – Instituto de Geociências, Universidade Paulista, Rio Claro.

Meira, V.T., García-Casco, A., Juliani, C., Almeida, R.P., and Schorscher, J.H.D., 2015, The role of intracontinental deformation in supercontinent assembly: insights from the Ribeira Belt, Southeastern Brazil (Neoproterozoic West Gondwana): Terra Nova, v. 27, p. 206-217, DOI:10.1111/ter.12149.

METAL MINING AGENCY of JAPAN. Japan International Cooperation Agency. 1981. Report on geological survey of Anta Gorda: Phase I. Tokyo, 1981. 79 f. Inclui mapas.

METAL MINING AGENCY of JAPAN. Japan International Cooperation Agency. 1982. Report on geological survey of Anta Gorda: Phase II. Tokyo, 1982. 3 v.

METAL MINING AGENCY of JAPAN. Japan International Cooperation Agency. 1983. Report on geological survey of Anta Gorda: phase III. Tokyo, 1983. 2 v.

METAL MINING AGENCY of JAPAN. Japan International Cooperation Agency. 1983. Report on geological survey of Anta Gorda: phase IV. São Paulo: CPRM, 1984. 2 v.

Morgental, A.; Batolla Júnior, F.; Pinto, G. G.; Paiva, I. P.; Drumond, J. B. V. Projeto Sudelpa: relatório final. São Paulo: SUDELPA/CPRM, 1975a.

Morgental, A.; Batolla Júnior, F.; Pinto, G. G.; Paiva, I. P.; Drumond, J. B. V. Projeto Sudelpa: fichas de ocorrências. São Paulo: SUDELPA/CPRM, 1975b.

Morgental, A.; Silva, A. A. G. P. da; Borin Júnior, T.; Alegri, V.; Oliveira, P. E. P. de. Projeto geoquímica no Vale do Ribeira: relatório final. São Paulo: DNPM/CPRM, 1978.

Morgental, A.; Paiva, I. P.; Borin Júnior, T.; Pinto, G. G.; Carmo, L. S. do. Pesquisa de ouro no Vale do Ribeira: atuação da CPRM. In: SIMPÓSIO REGIONAL DE GEOLOGIA, 3., 1981. Curitiba. Atas. Curitiba: SBG, 1981. p. 56-70.

Ohmoto, H., Rye, R.O., 1979. Isotopes of sulfur and carbon. In: Barnes, H.L. (Ed.), Geochemistry of Hydrothermal Ore Deposits. John Wiley & Sons, pp. 509e567.0Pokrovski, G.S., Dubrovinsky, L.S., 2011. The S3- ion is stable in geological fluids at elevated temperatures and pressures. Science 331, 1052e1054.

Paiva, I. P. and Morgental, A. Prospecto Ouro nas Regiões Auríferas dos Agudos Grandes e Morro do Ouro, Vale do Ribeira. São Paulo: CPRM, 1980.

Parr, J.M. and Plimer, 1.R., 1993. Models for Broken Hill Type lead-zinc-silver deposits. In: Kirkham, R.Y. , Sinclair, WD., Thorpe, R.1. and Duke, J.M. (editors), Mineral deposit modeling. Geological Association of Canada, Special Paper 40, 253-288.

Piekarz, G.F. 1981. Reconhecimento de Unidades Correlacionáveis à Seqüência Mineralizada do Perau, Estado do Paraná. Atas do 3° Simpósio Regional de Geologia - SBG/Núcleo de São Paulo, VoI. 1. pp. 148-154.

Prazeres Filho, H.J. Caracterização geológica e petrogenética do batólito granítico Três Córregos (PR-SP): geoquímica isotópica (Nd-Sr-Pb), idades (ID-TIMS/SHRIMP) e δ18O em zircão. 2005. 207 p. Tese (Doutorado) – Universidade de São Paulo, São Paulo, São Paulo, 2005.

Ramboz, C., Pichavant, M., and Weisbrod, A., 1982, Fluid immiscibility in natural processes: use and misuse of fluid inclusion data. II. Interpretation of fluid inclusion data in terms of immiscibility: Chemical Geology, v. 37, p. 29-48.

Ribeiro, L.M.A.L. Estudo geológico e geocronológico dos terrenos granito-gnáissicos e sequências metavulcanossedimentares da região do Betara, PR. 2006. Dissertação (Mestrado) – Instituto de Geociências, Universidade de São Paulo, São Paulo, 2006.

Rich, R.A. (1979) Fluid inclusion evidence of Silurian evaporites in southeastern Vermont, Geol. Soc. Am. Bull., 90, 901–2.

Rodrigues, S. W. de O; Caltabellotta, F. P.; Almeida, V. V.; Brumatti, M.; Archanjo, C. J.; Hollanda, M. H. B. M.; Salazar, C. A.; Liu, D. 2011. Petrografia, geoquímica e geocronologia dos granitos Patrimônio Santo Antônio e São Domingos (Suíte Cunhaporanga, Paraná, Sudeste do Brasil). Geologia USP - Série Científica, São Paulo, v.11, n. 3, p. 03-21, 2011.

Seccombe, P.K., 1977. Sulphur isotope and trace metal composition of stratiform sulphides as an ore guide in the Canadian Shield. J. Geochem. Explor. 8, 117–137.

Siga Junior, O.; Basei, M. A. S.; Sato, K.; Passarelli, C. R.; Nutman, A.; Mcreath, I.; Prazeres Filho, H. J. Calymmian (1.50 1.45 Ga) magmatic records in Votuverava and Perau sequences, south-southeastern Brazil: Zircon ages and Nd–Sr isotopic geochemistry. Journal of South American Earth Sciences, v. 32, p. 301–308. 2011.

Silva, A. D. R., Campos, F. F., Brumatti, M., Salvador, E. D., Pavan, M. Mineralizações polimetálicas (Pb-Zn-Ag-Cu-Ba) associadas à Formação Perau, Cinturão Ribeira Meridional: estado do Paraná. São Paulo, CPRM, 2019. 125 p.; 1 mapa color. (Informe de Recursos Minerais. Série Províncias Minerais do Brasil, 21).

Silva, Antero T.S.F. da *et al*. Projeto Integração e Detalhe Geológico no Vale do Ribeira: Relatório Final. São Paulo: CPRM, 1981 15 v.

Silva, C.R., Takahashi, A. T., Chiodi Filho, C., Batolla JR, F. 1982. Geologia e mineralizações da região Perau-Água Clara, Vale do Ribeira, PR. In: Congresso Brasileiro de Geologia, 32°, Salvador, SBG. Anais, v,3:1024-1036.

Soares, P. C. 1987. Sequências tecto-sedimentares e tectônica deformadora no centro-oeste do escudo paranaense. In: Simpósio Sul-Bras. Geol., 3°. Curitiba, SBG., Atas, v. 2:743-771.

Souza, I. M. 1972. Relatório dos trabalhos de pesquisa de cobre no Ribeirão Perau, município de Adrianópolis, PR. Eletro São Marcos Ltda/Sonda S/C, São Paulo, 41p. (inédito).

Span, R., and Wagner, W., 1996, A new equation of state for carbon dioxide covering the fluid region from the triple-point temperature to 1100 K at pressures up to 800 MPa: Journal of Physical and Chemical Reference Data, v. 25, p. 1509-1596.

Takahashi,A. T. ; Chiodi Filho, C.; Silva, C.R.; Batolla Jr., F. (1981) Projeto Integração e Detalhe Geológico no Vale do Ribeira. Relatório Final. Área da Mina do Perau. DNPM/CPRM, São Paulo, v. 11, 94 p.

Tassinari, C. C. G.; Barbour, A. P.; Daitx, E. C.; Sato. K. 1990. Aplicação dos isótopos de Pb e Sr na determinação da natureza das fontes das mineralizações de chumbo do Vale do Ribeira - SP e PR. In: CONGRESSO BRASILEIRO DE GEOLOGIA, 36. , 1990, Natal. Anais. Natal: Sociedade Brasileira de Geologia, 1990. V. 3, p. 1254-1266.

Touret, J.R.L. (1977) The significance of fluid inclusions in metamorphic rocks, in Thermodynamics in Geology (ed. D.G. Fraser). NATO ASI Series, D. Reidel Publ., pp. 203–27.

Wilkinson, Jamie. (2013). Sediment-Hosted Zinc-Lead Mineralization: Processes and Perspectives. Treatise on Geochemistry: Second Edition. Chapter 13. 219-249. 10.1016/B978-0-08-095975-7.01109-8.

Yogi, M. T., Faleiros, F. M., Laniri, P., Cabrita, D. Thermo-kinematic evolution of the Anta Gorda Anticlinorium, Ribeira Belt: metamorphism record and shear deformation in a transpressional setting. 2019. Geophysical Research Abstracts. Vol. 21, EGU2019-11840,2019. EGU General Assembly 2019.

Zhang, Y.G., and Frantz, J.D., 1987, Determination of the homogenization temperatures and densities of supercritical fluids in the system NaCl-KCl-CaCl2-H2O using synthetic fluid inclusions: Chemical Geology, v. 64, p. 335-350.